

UC Berkeley

Faculty Research

Title

Morning Commute in a Single-Entry Traffic Corridor with No Late Arrivals

Permalink

<https://escholarship.org/uc/item/1h2604ft>

Authors

DePalma, Elijah
Arnott, Richard

Publication Date

2011-02-04

University of California Transportation Center
UCTC-FR-2011-20

**Morning Commute in a Single-Entry Traffic Corridor
with No Late Arrivals**

Elijah DePalma and
Richard Arnott
University of California, Riverside
September 2011

Morning Commute in a Single-Entry Traffic Corridor with No Late Arrivals

Elijah DePalma

Department of Statistics, University of California, Riverside
Riverside, CA 92506, *edepalma@math.ucr.edu*, (951)234-2190

Richard Arnott

Department of Economics, University of California, Riverside
Riverside, CA 92506, *richard.arnott@ucr.edu*, (951)827-1581

February 4, 2011

Abstract

This paper analyzes a model of early morning traffic congestion, that is a special case of the model considered in Newell (1988). A fixed number of identical vehicles travel along a single-lane road of constant width from a common origin to a common destination, with LWR flow congestion and Greenshields' Relation. Vehicles have a common work start time, late arrivals are not permitted, and trip cost is linear in travel time and time early. The paper explores traffic dynamics for the Social Optimum, in which total trip cost is minimized, and for the User Optimum, in which no vehicle's trip cost can be reduced by altering its departure time. Analytical and, when possible, closed-form solutions are presented, along with numerical examples.

Keywords: corridor, morning commute, social optimum, user optimum

1 Introduction ¹

In recent years considerable theoretical work has been done on the dynamics of rush-hour traffic congestion. Most of this work has applied the basic bottleneck model (Vickrey (1969), as simplified in Arnott, de Palma and Lindsey (1990)), in which congestion takes the form of a queue behind a single bottleneck of fixed flow capacity. A strength of the bottleneck model is its simplicity, which permits many extensions. A weakness is that the technology of traffic congestion may not be well described by queues behind bottlenecks. This paper replaces bottleneck congestion with LWR (Lighthill and Whitham (1955) and Richards (1956)) flow congestion, which combines the equation of continuity (conservation of mass for a fluid) with an assumed technological relationship between local velocity and local traffic density, and covers bottleneck congestion as a limiting case.

Newell (1988) (herein referred to as Newell) considered a model of the morning commute in which a fixed number of identical commuters must travel along a road of constant width subject to LWR flow congestion, from a common origin to a common destination, and in which trip costs are a linear function of travel time and schedule delay. He allowed for a general distribution of desired arrival times and a general technological relationship between local velocity and local density, and precluded late arrivals by assumption. He obtained qualitative properties of both the social optimum (SO) in which total trip cost is minimized, and the user optimum (UO) in which no commuter can reduce their trip cost by altering their departure time. While a tour de force, his paper has been overlooked by the literature, likely because of the density of its discussion and analysis.

Our paper provides a detailed analysis of a special case of Newell's model, assuming that commuters have a common desired arrival time and that local velocity is a negative linear function of local density (Greenshields' Relation). It complements Newell's paper in three

¹Richard Arnott thanks the US Department of Transportation, grant #DTRT07-G-0009, and the California Department of Transportation, grant #65A0216, through the University of California Transportation Center (UCTC) at UC Berkeley. Elijah DePalma thanks the University of California Transportation Center (UCTC) for the dissertation fellowship award.

respects. First, it is more accessible, laying down arguments in greater detail and providing numerical solutions. Second, by restricting the analysis to Greenshields' Relation, the paper obtains a closed-form solution to the SO problem, and a complete analytical solution to the UO problem, which provide additional insight. Third, unlike Newell, it discusses economic properties of the solutions.

We came to the topic of this paper indirectly. Interested in the spatial-temporal dynamics of rush-hour traffic congestion in a metropolitan area, Arnott posed the Corridor Problem, which is identical to the model considered in this paper except that traffic enters at all locations along the road. In the process of studying the Corridor Problem (Arnott and DePalma (2010) gives some preliminary results), Arnott and DePalma came to appreciate its difficulty, and decided to investigate a sequence of simpler problems, the first having cars enter at only one location. Thus, the problem addressed in this paper might be termed the *Single-Entry Corridor Problem*.

Section 2 presents the model and notation, introduces the components of LWR traffic flow theory used in the paper, and illustrates how they are applied by solving for the traffic dynamics along a uniform point-entry, point-exit road, in response to an increase in the entry rate from zero to a constant level for a fixed time period. Sections 3 and 4 contain the main results of the paper, presenting the SO and UO solutions respectively. Section 5 investigates the model's economic properties, and contrasts them with those of the bottleneck model. Section 6 discusses directions for future research and concludes.

2 Model Description

Consider a road of constant width that connects a single entry point to a point central business district (CBD) that lies at the eastern end of the corridor. Since the primary results of this paper are derived from Newell, we adopt the notation and terminology used there, with the following exception: We use the word *departure* to indicate a vehicle's departure

from the origin and consequent entry into the corridor, and the word *arrival* to indicate a vehicle's arrival at the CBD and consequent exit from the corridor, whereas Newell uses these words in the opposite manner².

Location is indexed by x , with the entry point located at $x = 0$ and the CBD at $x = l$. The corridor consists of a road from $x = 0$ to $x = l$, and possibly a queue at $x = 0$ as well. At time t , let $A(t)$ denote the cumulative inflow into the corridor (including those that may be in a queue), $A_R(t)$ the cumulative inflow into the road, and $Q(t)$ the cumulative outflow at $x = l$. Let $a(t) = \frac{dA}{dt}$ denote the inflow rate into the corridor, $a_R(t) = \frac{dA_R}{dt}$ the inflow rate into the road, and $q(t) = \frac{dQ}{dt}$ the outflow rate at $x = l$.

Let N denote population, t_f the time of the last vehicle departure into the corridor, t_R the time of the last vehicle departure into the road, and \bar{t} the time of the last vehicle arrival at the CBD. If a queue is present at time t_f , then $t_R > t_f$. We will normalize time such that the first departure occurs at time $t = 0$; consequently, t_f , t_R and \bar{t} are endogenous times that provide alternative measures of the duration of the morning rush hour and are not specified *a priori*.

2.1 Trip Cost

All vehicles have a common desired arrival time, the work start-time, which coincides³ with the time of the last vehicle arrival, \bar{t} .

Let $\tau(t)$ denote the travel time of the vehicle departing at time t (which includes time spent in a queue), α_1 the per unit cost of travel time, α_2 the per unit cost of schedule delay

²As indicated in Lago and Daganzo (2007), in queueing theory it is customary to use the terms *arrivals* to and *departures* from a server, whereas in the economics literature the terms are used in reverse, referring to *departures* from an origin and *arrivals* at a destination.

³The final departure at time t_f arrives at the CBD at time \bar{t} . Since late arrivals are not permitted, \bar{t} cannot occur later than the work start-time. If \bar{t} occurs earlier than the work start-time, then a constant schedule delay cost will be added to each vehicle's trip cost, which can be eliminated without changing the traffic dynamics by uniformly translating the entire system in time so that \bar{t} coincides with the work start-time.

(i.e., time early arrival), and $C(t)$ the trip cost:

$$\begin{aligned} \text{Trip Cost} &= \text{Travel Time Cost} + \text{Schedule Delay Cost} \\ C(t) &= \alpha_1 \tau(t) + \alpha_2 (\bar{t} - [t + \tau(t)]), \quad 0 \leq t \leq t_f. \end{aligned} \tag{2.1.1}$$

Denote the sum of all trip costs as the *total trip cost*, TTC :

$$\begin{aligned} \text{Total Trip Cost} &= \text{Total Travel Time Cost} + \text{Total Schedule Delay Cost} \\ TTC &= \alpha_1 (\text{Total Travel Time}) + \alpha_2 (\text{Total Schedule Delay}) \\ &= \alpha_1 \int_0^{t_f} \tau(t) a(t) dt + \alpha_2 \int_0^{t_f} (t^* - [t + \tau(t)]) a(t) dt. \end{aligned} \tag{2.1.2}$$

Throughout this paper we assume that $\alpha_1 > \alpha_2$, which is supported by empirical evidence in Small (1982), and which is a necessary condition for constructing a UO solution, as is explained in a more general setting in Section 4 of Newell.

2.2 Traffic Dynamics

Following Newell, let $k(x, t)$, $v(x, t)$ and $q(x, t)$ ⁴ denote traffic density, velocity and flow, respectively. As does most of the literature, we assume that the velocity-density relationship has the following features:

- v achieves a maximum value of v_0 (free-flow velocity) when $k = 0$.
- v is a non-increasing function of k and equals zero when $k = k_j$ (jam density).
- q achieves a maximum value of q_m (capacity flow) at a unique density value, $k = k_m$.
- q is an increasing function of k for $0 \leq k \leq k_m$ (ordinary flow).
- q is a decreasing function of k for $k_m \leq k \leq k_j$ (congested flow).

⁴As in Newell, the symbol q has different interpretations depending on context: i) $q(x, t)$ denotes the flow rate at the spacetime point (x, t) ; ii) $q(t)$ denotes the outflow rate out at $x = l$; iii) q denotes the flow rate used as a dependent or independent variable with other quantities, such as v and k .

Throughout the paper all analytic results are derived using Greenshields' Relation, i.e., the linear velocity-density relationship, $\frac{v}{v_0} = 1 - \frac{k}{k_j}$ (see A-1).

2.2.1 Continuity Equation, Characteristics and Shocks

The continuity equation, its solution using the method of characteristics, and the formation of shock and rarefaction waves, are explained in detail in books such as Matheij and Rienstra (2005). Here we briefly sketch the concepts that are relevant to our paper.

The LWR traffic flow model is formulated in terms of a hyperbolic partial differential equation known as the continuity equation, which is a statement of conservation of mass of a fluid:

$$\frac{\partial k(x, t)}{\partial t} + \frac{\partial q(x, t)}{\partial x} = 0.$$

Inserting a functional relationship between flow and density, $q(k)$, into the continuity equation yields

$$\frac{\partial k(x, t)}{\partial t} + q'(k) \frac{\partial k(x, t)}{\partial x} = 0. \quad (2.2.1)$$

The method of characteristics for solving (2.2.1) is to reduce the PDE to a pair of ODE's:

i) $\frac{dx}{dt} = q'(k(x, t))$; and ii) $\frac{dk(x, t)}{dt} = 0$. The solutions to this pair of ODE's are called *characteristic curves*, or *characteristics*, and are straight lines in the spacetime plane along which k is constant. In t - x space, a characteristic line with density k has slope $\frac{\Delta x}{\Delta t} = q'(k)$, which is termed its wave velocity. As in Newell, it is more convenient to work in x - t space and to deal with the reciprocal of the wave velocity normalized by free-flow velocity, $w = \frac{v_0}{q'(k)}$. Greenshields' Relation yields $w = \frac{1}{1 - \frac{k}{k_m}}$, and in the ordinary flow régime, $k \leq k_m$, we can write w in terms of q as

$$w = \frac{1}{\sqrt{1 - \frac{q}{q_m}}}. \quad (2.2.2)$$

When characteristic lines intersect, the density becomes discontinuous, resulting in what is called a *shock wave*, which propagates through spacetime along a curve called the *shock wave path*, i.e., a path of intersecting characteristic lines. Although the continuity equation,

(2.2.1), is not satisfied along a shock wave path, a weak, integral-form of the continuity equation is satisfied. However, to uniquely determine a solution to the weak form of the continuity equation an additional condition is required, called the *entropy condition*.⁵ This condition requires that, for fixed t , as x increases from left to right across a shock wave path the density across the shock wave path must discontinuously increase, i.e., $k_l < k_r$, where k_l is the density to the left of the shock wave path and k_r is the density to the right of the shock wave path. As shown in Matheij and Rienstra (2005), the speed of the shock wave path must satisfy

$$\left(\frac{dx}{dt}\right)_{\text{Shock}} = \frac{q_r - q_l}{k_r - k_l}, \quad (2.2.3)$$

where flows q_l and q_r are defined similarly to k_l and k_r .

2.2.2 Trajectory of Last Vehicle Departure is a Shock Wave Path

If the last vehicle to depart does not travel at free-flow velocity, then its trajectory coincides with a shock wave path. To see this, consider a point on the trajectory of the last vehicle to depart. For fixed t , to the left of this point flow and density are both zero, whereas to the right flow and density are both greater than zero, $q_r > 0$ and $k_r > 0$, so that the point lies on a shock wave path. Since, from (2.2.3), the speed of the shock wave at this point is $\frac{q_r}{k_r}$, which coincides with the velocity of the vehicle at this point, the vehicle's trajectory is a shock wave path.

2.2.3 Corridor and Road Inflow Rates, and Queue Development

Since the inflow rate into the road cannot exceed capacity flow, a queue develops if and only if the inflow rate into the corridor, $a(t)$, is greater than capacity flow. If a queue is present, then the inflow rate into the road, $a_R(t)$, is capacity flow. Furthermore, since entries do not occur at any other point along the road, the traffic dynamics along the road will be in the

⁵As discussed in Section 4.4.2 of Daganzo (1997), the entropy condition is equivalent to requiring that each interior spacetime point be connected to a point on the boundary through a truncated characteristic which does not intersect any other characteristics or shocks.

ordinary flow régime for all time.

2.2.4 Method of Characteristics for the Single-Entry Corridor Problem

The following discussion is relevant to Figures 2.1, 3.3 and 4.3. Given a road inflow rate, $a_R(t)$ for $0 \leq t \leq t_R$, to determine the traffic dynamics throughout spacetime we draw a half-line characteristic emanating from each point $(0, t)$ on the t -axis with slope $\frac{\Delta t}{\Delta x} = \frac{1}{v_0 \sqrt{1 - \frac{a_R(t)}{q_m}}}$. Along this line density, flow and velocity are all constant, with flow being the constant value $a_R(t)$, and density and velocity being derived from the flow value via Greenshields' Relation. Provided that this line does not intersect any other characteristic line, the density along this line is constant from $x = 0$ to $x = l$.

In spacetime regions of zero density the characteristic lines have slope $\frac{1}{v_0}$ and coincide with vehicle trajectory curves corresponding to free-flow travel. Since the corridor is initially empty, the first vehicle departure at $t = 0$ travels at free-flow velocity, arriving at the CBD at time $t = \frac{l}{v_0}$.

If the inflow rate discontinuously increases at a point in time, then the slope of the characteristic lines emanating just below and just above that point on the t -axis also discontinuously increases. A fan of characteristic lines emanates from this point, referred to as a *rarefaction wave*.

After drawing all characteristics and determining all shock paths, density is determined for all spacetime points (x, t) , $0 \leq x \leq l$ and $-\infty < t < \infty$. Using Greenshields' Relation we can determine the velocity at each spacetime point, from which we can obtain vehicle trajectory curves and trip costs. Although this solution method works in principle, it is computationally difficult to calculate shock paths; however, some recent work has been done in designing a robust algorithm for use with Greenshields' Relation, Wong and Wong (2002). A much simpler method is to use the cell-transmission model, (Daganzo (1995)), which uses a finite-difference-equation approximation to the continuity equation to determine the density at all spacetime points. The cell-transmission model does not permit the exact solution

of shock wave paths, but given *any* initial inflow rate and *any* flow-density relationship, it permits numerical determination of the outflow rate, trajectory curves and trip costs. Throughout the paper we have repeatedly used the cell-transmission model to numerically verify the theoretically derived results.

2.2.5 Cumulative Inflow and Outflow Curves

The following discussion is relevant to Figures 2.2, 2.4, 3.1, 3.2 and 4.2. Section 2 of Newell determines relations which, in the absence of shocks, must be satisfied by cumulative inflow and outflow curves, and we restate those relations here. Let $(t, A(t))$ and $(t', Q(t'))$ be points on the cumulative inflow and outflow curves, respectively, such that the flow rates at both points are equal, i.e., $a(t) = q(t')$. These two points are related via equations (2.7) and (2.14) from Newell:

$$t = t' - \frac{l}{v_0}w(q) \tag{2.2.4a}$$

$$A(t) = Q(t') - \frac{l}{v_0}q \left[w(q) - \frac{v_0}{v(q)} \right], \tag{2.2.4b}$$

where $w(q)$ is given in (2.2.2). In a graph of cumulative inflow and outflow curves, we use a dashed line to connect these related points of equal flow rate, and therefore these dashed lines have slope

$$\frac{Q(t') - A(t)}{t' - t} = q \left[1 - \frac{v_0}{w(q)v(q)} \right]. \tag{2.2.5}$$

2.3 Scaled Units

Throughout the paper we utilize the following system of scaled units:

- Choose length units such that $l = 1$.
- Choose time units such that $\frac{l}{v_0} = 1$, so effectively $v_0 = 1$.

- Choose population units such that $\frac{q_m l}{v_0} = 1$, so effectively $q_m = 1$. Under Greenshields' Relation, this choice of population units is equivalent to $k_j = 4$.
- Choose cost units such that $\alpha_1 \frac{q_m l}{v_0} \frac{l}{v_0} = 1$, so effectively $\alpha_1 = 1$.

Given an equation in scaled units, we can recover the unscaled equation by dividing each term by the appropriate scaling factor. For example, in the SO we determine the time of the last vehicle arrival at the CBD in scaled units:

$$\bar{t} = 1 + \frac{1}{2}N + \sqrt{\frac{1}{\alpha_2}N + \left(\frac{1}{2}N\right)^2}.$$

Since \bar{t} has units of time, N has units of population and α_2 has units of cost per population per time, to recover the unscaled equation we replace \bar{t} with $\frac{\bar{t}}{v_0}$, N with $\frac{N}{q_m l}$, and α_2 with $\alpha_2 \frac{q_m l}{v_0} \frac{l}{v_0} = \frac{\alpha_2}{\alpha_1}$. Inserting these replacements into the previous equation yields

$$\bar{t} = \frac{l}{v_0} + \frac{1}{2} \frac{N}{q_m} + \sqrt{\frac{\alpha_1}{\alpha_2} \frac{l}{v_0} \frac{N}{q_m} + \left(\frac{1}{2} \frac{N}{q_m}\right)^2}.$$

Unless otherwise specified, all of the results which follow are in scaled units.

2.4 Constant Inflow Rate

In this section we analyze the traffic dynamics resulting from a constant inflow rate into the corridor, $a(t) = q_c$ from $t = 0$ to $t = t_f$. We analytically derive vehicle trajectories and their associated trip costs, the outflow rate, and total trip cost.

If $q_c > 1$, a queue develops at the entry point and the road inflow rate is capacity flow, 1. In this case, for $t > t_f$ the corridor inflow ceases, the queue dissipates, and the road inflow rate is capacity inflow until time $t_R > t_f$, at which point the entire population has entered the road. The resulting traffic dynamics are identical to a situation in which an identical size population enters the corridor at capacity inflow from $t = 0$ to $t = t_R$. The

only differences between the two situations are the individual vehicle trip costs and total trip cost, since in the former situation vehicles in a queue incur an additional travel time cost. In the following derivations we initially presume that the constant inflow rate satisfies $q_c \leq 1$, and later remark on how total trip cost is affected if $q_c > 1$.

2.4.1 Characteristic Curves

Vehicles depart at a constant inflow rate, $q_c \leq 1$, during the time interval $0 \leq t \leq t_f$. Since a population N departs, $t_f = \frac{N}{q_c}$. For $t < 0$ and $t > t_f$ the characteristic lines emanating from the t -axis have slope 1, representing free-flow traffic, and for $0 < t < t_f$ the characteristic lines have slope $w_c = \frac{1}{\sqrt{1-q_c}} > 1$. Thus, at $t = 0$ we obtain a rarefaction wave, and at $t = t_f$ we obtain a shock wave whose path coincides with the trajectory of the last vehicle departure. The following analysis is split into two separate cases:

Case 1 All vehicle trajectories intersect the rarefaction wave.

Case 2 Not all vehicle trajectories intersect the rarefaction wave.

Vehicles departing at time $t > 0$ travel with constant velocity

$$v_c = \frac{1 + \sqrt{1 - q_c}}{2} = \frac{w_c + 1}{2w_c},$$

until reaching either the upper boundary of the rarefaction wave (Cases 1 and 2) or the CBD (Case 2 only). Since the upper boundary line of the rarefaction wave has slope w_c , the time point at which the upper boundary line reaches the CBD is w_c . Let t_c denote the departure time of a vehicle that would reach the CBD at time w_c if it traveled at constant velocity v_c , so that

$$t_c = w_c - \frac{1}{v_c} = \frac{w_c(w_c - 1)}{w_c + 1}.$$

Thus, a vehicle departing earlier than t_c travels at constant velocity v_c until reaching the upper boundary of the rarefaction wave (Cases 1 and 2), whereas a vehicle departing later

than t_c travels at constant velocity v_c until reaching the CBD (Case 2 only). Case 1 occurs if $t_f \leq t_c$, or, equivalently, $\frac{N}{q_c} \leq \frac{w_c(w_c-1)}{w_c+1}$. Since $w_c = \frac{1}{\sqrt{1-q_c}}$, this condition reduces to

$$q_c \geq 1 - \frac{1}{\left(1 + \frac{N}{2} + \sqrt{N + \left(\frac{N}{2}\right)^2}\right)^2}. \quad (\text{Case 1})$$

Thus, Case 1 occurs if the inflow rate q_c is sufficiently large relative to the population. Figure 2.1 plots characteristic lines and the trajectory of the final vehicle departure for Cases 1 and 2.

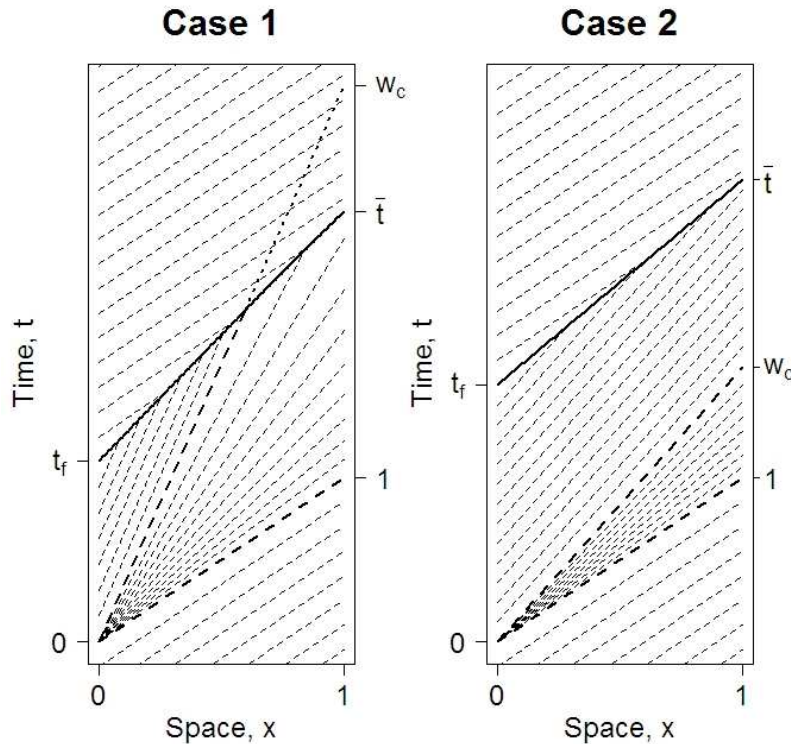


Figure 2.1: Dashed lines are characteristics corresponding to a constant inflow rate from $t = 0$ to $t = t_f$, and the solid line is the trajectory of the final vehicle departure. The bold, dashed lines are characteristics corresponding to the boundaries of the rarefaction wave arising from the initial discontinuous increase in the inflow rate. Case 1 occurs if the inflow rate is sufficiently large relative to the population. In Case 1 the upper boundary of the rarefaction wave does not reach the CBD since it intersects the shock wave corresponding to the trajectory of the final vehicle trajectory, although we indicate its intended path using a dotted line.

2.4.2 Vehicle Trajectories

Denote the departure time of a vehicle as t_d , $0 \leq t_d \leq t_f$, and its arrival time as t_a , $1 \leq t_a \leq \bar{t}$. The first vehicle departure occurs at $t_d = 0$, with corresponding arrival at $t_a = 1$, and its trajectory is a straight line coinciding with the lower boundary of the rarefaction wave. If $t_d > 0$, then the vehicle initially travels at constant velocity $v_c = \frac{w_c+1}{2w_c}$, so that the trajectory is a straight line whose spacetime coordinates, (x, t) , satisfy

$$x(t) = \frac{w_c + 1}{2w_c}(t - t_d).$$

If $t_d \geq t_c$ (Case 2 only), then the vehicle's straight-line trajectory arrives at the CBD at time

$$t_a = t_d + \frac{2w_c}{w_c + 1}.$$

If $t_d < t_c$ (Cases 1 and 2), then the vehicle's straight-line trajectory intersects the upper boundary of the rarefaction wave at the spacetime point

$$(x_0, t_0) = \left(t_d \frac{w_c + 1}{w_c(w_c - 1)}, t_d \frac{w_c + 1}{w_c - 1} \right).$$

Upon entering the interior of the rarefaction wave the vehicle's speed at a spacetime point depends upon the flow value at that spacetime point through Greenshields' Relation, and the flow value at that spacetime point is determined by the characteristic line upon which it lies. If we denote the spacetime point of the vehicle trajectory as (x, t) , then since the characteristic line along which it lies is generated from a fan of characteristic lines emanating from the origin, the flow along the characteristic line, q , satisfies $\frac{1}{\sqrt{1-q}} = \frac{t}{x}$. From Greenshields' Relation (A-1) the vehicle's speed satisfies $v = \frac{1}{2} [1 + \sqrt{1-q}]$, and combining these two equations yields a differential equation for the vehicle's trajectory curve in the interior of the rarefaction wave:

$$\frac{dx}{dt} = \frac{1}{2} \left[1 + \frac{x}{t} \right]. \quad (2.4.1)$$

This equation can be solved by making the substitution $y = \frac{x}{t}$, resulting in the general solution $x(t) = t + A\sqrt{t}$, where A is an arbitrary constant determined from the initial condition that the trajectory curve originates from the spacetime point (x_0, t_0) . After some algebraic simplifications we obtain the trajectory within the interior of the rarefaction wave as

$$x(t) = t - \sqrt{t_d q_c} \sqrt{t},$$

which arrives at the CBD at time

$$t_a = 1 + \frac{t_d q_c}{2} + \sqrt{t_d q_c + \left[\frac{t_d q_c}{2} \right]^2}.$$

In Table 1 we summarize, providing expressions for the vehicle trajectories and their arrival times in terms of their departure times, t_d . The last departure occurs at time $t_f = \frac{N}{q_c}$, and arrives at time \bar{t} . Replacing t_d with t_f in the arrival time expressions determines \bar{t} for Cases 1 and 2, and these results are also provided in Table 1.

2.4.3 Outflow Rate

Figure 2.1 provides a graphical method to determine the outflow rate at the CBD, $q(t)$, by determining the constant flow value on each characteristic line. The characteristic lines corresponding to free-flow travel have zero flow value, so that $q(t) = 0$ for $t < 1$ or $t > \bar{t}$. The characteristic lines that are generated from the rarefaction wave at the origin have flow value q and slope $w = \frac{1}{\sqrt{1-q}} = \frac{t}{1}$, so that $q(t) = 1 - \frac{1}{t^2}$ for $1 < t < \bar{t}$ (Case 1) and $1 < t < w_c$ (Case 2). We conclude that the outflow rate in this time period depends only upon the existence of a discontinuity in the inflow rate at the origin, and does not depend upon the magnitude of the discontinuity, q_c . In Case 2, for $w_c < t < \bar{t}$ the outflow rate is q_c . Integrating $q(t)$ yields the cumulative outflow curve, $Q(t)$. These results are summarized in Table 1.

In Figure 2.2 we plot the cumulative inflow and outflow curves for Cases 1 and 2. The dashed lines are constant-flow lines (whose slope is determined from (2.2.5)), and show how

the inflow generates the outflow. In Case 1 the cumulative outflow curve is generated by the initial discontinuity in the inflow rate, and the subsequent inflow does not affect the outflow rate. In Case 2 the first portion of the cumulative outflow curve from time $t = 1$ to $t = w_c$ is generated by the initial discontinuity in the inflow rate, and the second portion of the cumulative outflow curve from $t = w_c$ to $t = \bar{t}$ is generated by the inflow from $t = 0$ up to some point in time, which we denote as t' . The subsequent inflow after $t = t'$ does not affect the outflow rate.

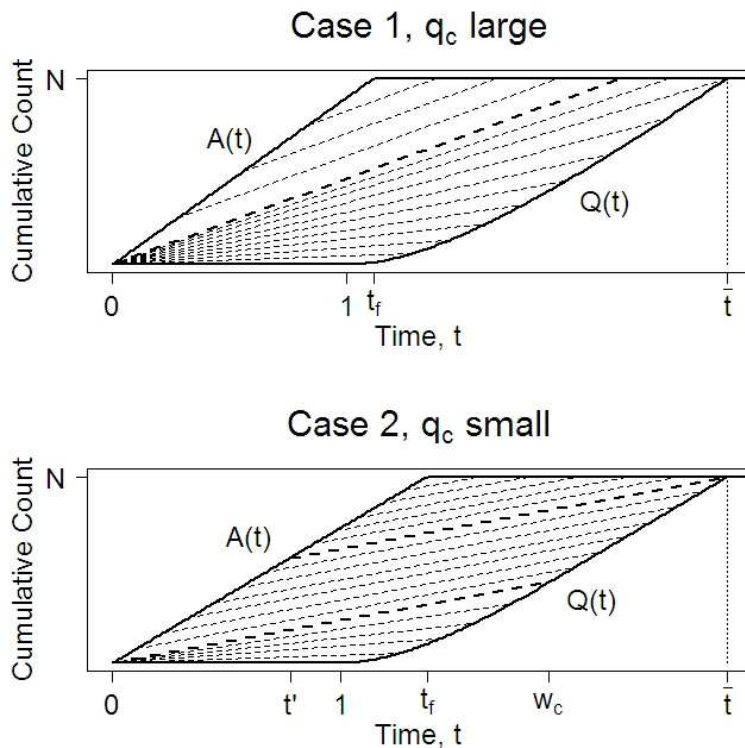


Figure 2.2: Sample cumulative outflow curves corresponding to a constant inflow rate for Cases 1 and 2. The dashed lines are constant flow lines, and show how the inflow generates the outflow. Note that in Case 1 the outflow is completely determined by a portion of the rarefaction wave arising from the initial discontinuity in the inflow rate, and does not depend upon the magnitude of the inflow rate, q_c .

2.4.4 Trip Costs

For a departure at time t_d , the travel time cost is $t_a - t_d$, schedule delay cost is $\alpha_2(\bar{t} - t_a)$, and trip cost is $C = t_a - t_d + \alpha_2(\bar{t} - t_a)$. In Figure 2.3 we graph these costs as functions of departure time for capacity inflow and $\alpha_2 = 0.5$.

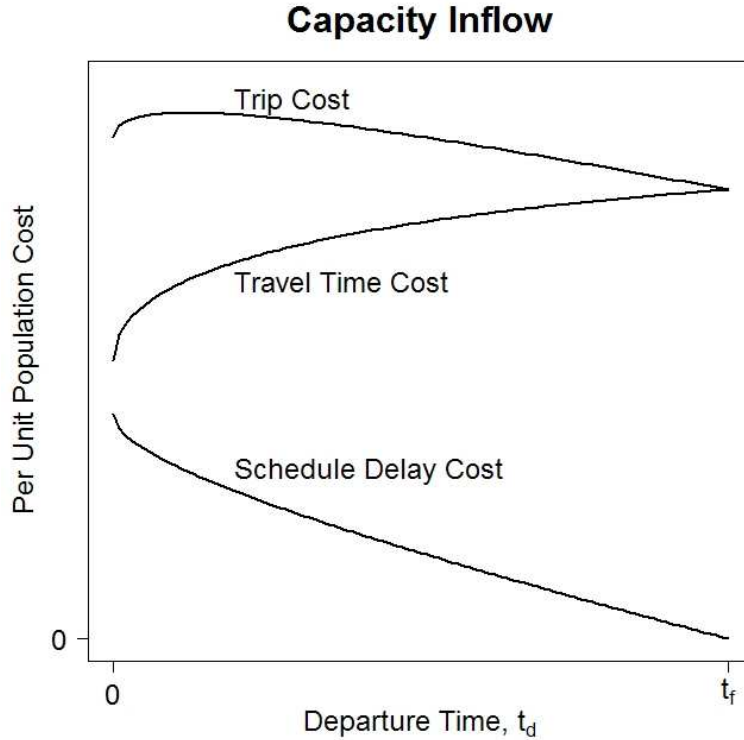


Figure 2.3: Schedule delay cost, travel time cost and trip cost as functions of departure time for capacity inflow rate, with $N = 1$ and $\alpha_2 = 0.5$ (Case 1 applies).

In Figure 2.2 the total schedule delay is the area under the cumulative outflow curve from $t = 1$ to $t = \bar{t}$,

$$\text{Total Schedule Delay} = \int_1^{\bar{t}} Q(t) dt, \quad (2.4.2)$$

the total travel time is the area between the cumulative inflow and outflow curves,

$$\text{Total Travel Time} = \int_0^{t_f} A(t) dt + N(\bar{t} - t_f) - \int_1^{\bar{t}} Q(t) dt, \quad (2.4.3)$$

and the total trip cost is

$$TTC = \text{Total Travel Time} + \alpha_2 (\text{Total Schedule Delay}). \quad (2.4.4)$$

Since $A(t) = q_c t$ for $0 < t < t_f$, using the expression for $Q(t)$ given in Table 1, we analytically determine the total schedule delay, total travel time and total trip cost, which are also provided in Table 1.

2.4.5 Queue Development

Suppose that a population of size N enters the corridor at an inflow rate greater than capacity flow, $q_c > 1$. Since the inflow into the road cannot exceed capacity flow, a queue develops at the entry point. The road inflow rate remains constant at capacity inflow until the queue has dissipated. Thus, the total population enters the corridor by time $t_f = \frac{N}{q_c}$, but does not enter the road until the later time, $t_R = \frac{N}{1} = N$. We can write the cumulative inflow curve into the corridor as

$$A(t) = q_c t, \quad 0 \leq t \leq t_f,$$

and the cumulative inflow curve into the road as

$$A_R(t) = t, \quad 0 \leq t \leq t_R.$$

The resulting traffic dynamics along the road are identical to a situation in which the total population enters the corridor at capacity inflow from $t = 0$ to $t = N$. However, queueing time adds to travel time. In Figure 2.4 we plot the cumulative corridor and road inflow curves, along with the cumulative outflow curve. The traffic dynamics along the road are determined by the inflow rate into the road, indicated by the lightly dashed lines. For a departure at time t , the horizontal distance between the cumulative corridor and road inflow curves is $q_c(t - 1)$, which is the queueing time. The total queueing time is the area between

	Case 1: $t_f \leq t_c \Leftrightarrow q_c$ large	Case 2: $t_f > t_c \Leftrightarrow q_c$ small
	$t_c = \frac{w_c(w_c-1)}{w_c+1}$, where $w_c = \frac{1}{\sqrt{1-q_c}}$	
Inflow Rate, q_c	$q_c \geq 1 - \frac{1}{\left(1 + \frac{N}{2} + \sqrt{N + \left(\frac{N}{2}\right)^2}\right)^2}$	$0 < q_c < 1 - \frac{1}{\left(1 + \frac{N}{2} + \sqrt{N + \left(\frac{N}{2}\right)^2}\right)^2}$
Arrival Time if $0 \leq t_d \leq t_c$	$t_a = 1 + \frac{t_d q_c}{2} + \sqrt{t_d q_c + \left[\frac{t_d q_c}{2}\right]^2}$	
Vehicle Trajectory if $0 \leq t_d \leq t_c$	$x(t) = \begin{cases} \left(\frac{w_c+1}{2w_c}\right)(t - t_d), & t_d \leq t \leq t_d \left(\frac{w_c+1}{w_c-1}\right) \\ t - \sqrt{t_d q_c} \sqrt{t}, & t_d \left(\frac{w_c+1}{w_c-1}\right) < t \leq t_a \end{cases}$	
Arrival Time if $t_d > t_c$	-	$t_a = t_d + \frac{2w_c}{1+w_c}$
Vehicle Trajectory if $t_d > t_c$	-	$x(t) = \left(\frac{w_c+1}{2w_c}\right)(t - t_d), \quad t_d \leq t \leq t_a$
Time of Last Vehicle Arrival	$\bar{t} = 1 + \frac{N}{2} + \sqrt{N + \left(\frac{N}{2}\right)^2}$	$\bar{t} = \frac{N}{q_c} + \frac{2}{1+\sqrt{1-q_c}}$
Outflow Rate	$q(t) = \begin{cases} 0, & t \leq 1 \text{ or } t \geq \bar{t} \\ 1 - \frac{1}{t^2}, & 1 < t < \bar{t} \end{cases}$	$q(t) = \begin{cases} 0, & t \leq 1 \text{ or } t \geq \bar{t} \\ 1 - \frac{1}{t^2}, & 1 < t \leq w_c \\ q_c, & w_c < t \leq \bar{t} \end{cases}$
Cumulative Outflow Rate	$Q(t) = \begin{cases} 0, & t \leq 1 \\ t + \frac{1}{t} - 2, & 1 < t \leq \bar{t} \\ N, & t > \bar{t} \end{cases}$	$Q(t) = \begin{cases} 0, & t \leq 1 \\ t + \frac{1}{t} - 2, & 1 < t \leq w_c \\ (t - w_c)q_c + \frac{(w_c-1)^2}{w_c}, & w_c < t \leq \bar{t} \\ N, & t > \bar{t} \end{cases}$
Total Schedule Delay	$TSD = \frac{1}{2}(\bar{t}^2 - 1) - 2(\bar{t} - 1) + \log \bar{t}$	$TSD = \frac{1}{2}(w_c^2 - 1) \left(\frac{\bar{t}}{w_c}\right)^2 - 2(w_c - 1) \left(\frac{\bar{t}}{w_c}\right) + \log w_c$
Total Travel Time	$TTT = N\bar{t} - \frac{N^2}{2q_c} - TSD$	$TTT = N\bar{t} - \frac{N^2}{2q_c} - TSD$
Total Trip Cost	$TTC = N\bar{t} - \frac{N^2}{2q_c} - (1 - \alpha_2)TSD$	$TTC = N\bar{t} - \frac{N^2}{2q_c} - (1 - \alpha_2)TSD$

Table 1: Table of results for a constant inflow rate, q_c (scaled units).

the two cumulative inflow curves, $\frac{1}{2}N^2 \left(1 - \frac{1}{q_c}\right)$. Thus, for an inflow rate of $q_c > 1$, the total trip cost is greater than that with capacity flow by $\frac{1}{2}N^2 \left(1 - \frac{1}{q_c}\right)$.

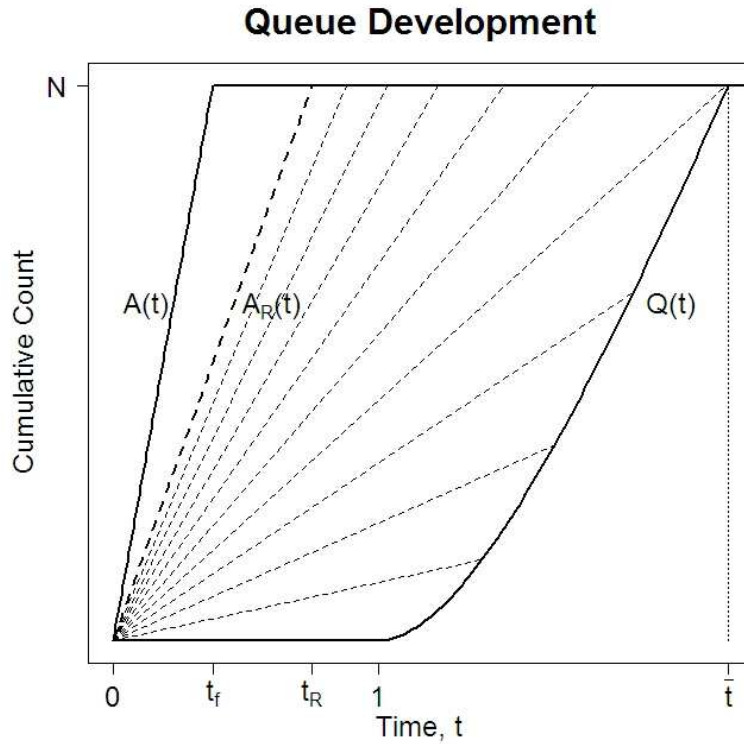


Figure 2.4: If the corridor inflow rate is greater than capacity inflow, then a queue develops and the road inflow rate equals capacity inflow for the duration of the queue. The traffic dynamics along the road are identical to the entire population entering at capacity inflow, but an additional total travel time is incurred equalling the area between the curves $A(t)$ and $A_R(t)$.

3 Social Optimum

Given population, N , and unit schedule delay cost, α_2 , the social optimum (SO) solution for the Single-Entry Corridor Problem with no late arrivals is the inflow rate function, $a(t)$, that minimizes total trip cost. Newell provides a method for constructing the solution for an arbitrary arrival demand curve. In this section we apply his results to the Single-Entry Corridor Problem in which the demand curve consists of zero arrivals before the work-start

time, \bar{t} , and the total population at the work-start time. As noted earlier, we normalize time so that the first departure occurs at $t = 0$; consequently, the length of the corridor rush hour, \bar{t} , is endogeneous.

3.1 Outflow Curve of Maximal Growth

Section 3 of Newell first determines the inflow rate function that minimizes total schedule delay, showing that the area under the cumulative outflow curve is minimized if $Q(t)$ is a cumulative outflow curve of maximal growth. To construct this curve, Newell first rewrites the flow-density relationship in terms of w instead of k to obtain flow as a function of w , $q^*(w)$, and subsequently determines the *nondimensional cumulative outflow curve of maximal growth*, denoted as $Q^*(w) = \int_1^w q^*(z) dz$. Greenshields' Relation, (2.2.2), allows Newell to determine

$$q^*(w) = 1 - \frac{1}{w^2},$$

from which Newell obtains

$$Q^*(w) = \int_1^w q^*(z) dz = w + \frac{1}{w} - 2. \quad (3.1.1)$$

Section 2 of Newell outlines a geometric procedure for constructing the cumulative outflow curve of maximal growth, $Q(t')$, using $Q^*(w)$. In this procedure, a segment of the Q^* curve must be drawn so that it is tangent to the (scaled) arrival-demand curve at some time t'_0 , and intersects the arrival-demand curve at some later time. Equation (2.12) from Newell determines the cumulative outflow curve, restated here using our scaled units:

$$Q(t') = Q(t'_0) + Q^*(w_0 + t' - t'_0) - Q^*(w_0). \quad (3.1.2)$$

In the Single-Entry Corridor Problem, the arrival-demand curve is a horizontal line with value zero for $t < \bar{t}$, and a horizontal line with value N for $t \geq \bar{t}$. Thus, the Q^* curve must

be drawn with slope zero at $(t'_0, 0)$, and must intersect the (scaled) arrival-demand curve at (\bar{t}, N) . The first condition implies that $q(t'_0) = 0$, so $w_0 = 1$. Since the first departure travels at free-flow velocity, the first arrival occurs at time $t'_0 = 1$. Inserting these values and (3.1.1) into (3.1.2) yields the cumulative outflow curve of maximal growth,

$$Q(t') = t' + \frac{1}{t'} - 2, \quad 1 \leq t' \leq \bar{t}, \quad (3.1.3)$$

where \bar{t} is determined such that $Q(\bar{t}) = N$. (3.1.3) is identical to the cumulative outflow rate for Case 1 in Table 1, which is generated as a result of a sufficiently large discontinuous increase in the inflow rate. Thus, the cumulative outflow curve of maximal growth, (3.1.3), does not uniquely generate an inflow rate. However, as indicated at the end of Section 2 in Newell, since the outflow rate at \bar{t} discontinuously drops to zero, a cumulative inflow curve can be uniquely generated as a backwards fan of waves originating from the point of discontinuous decrease in outflow rate. Specifically, let $(t, A(t))$ be a point on the cumulative inflow curve generated from a backwards fan of waves emanating from the discontinuity in the outflow rate at (\bar{t}, N) on the cumulative outflow curve. From (2.2.4a) we obtain:

$$t = \bar{t} - \frac{1}{\sqrt{1 - a(t)}} \quad \Rightarrow \quad a(t) = 1 - \frac{1}{(\bar{t} - t)^2}. \quad (3.1.4)$$

Since $A(0) = 0$, we can integrate $a(t)$ to determine $A(t)$,

$$A(t) = N - \left(\bar{t} - t + \frac{1}{\bar{t} - t} - 2 \right) \quad \text{for } 0 \leq t \leq t_f, \quad (3.1.5)$$

and $A(t_f) = N$ implies $t_f = \bar{t} - 1$. In Figure 3.1 we graph the cumulative outflow curve of maximal growth, along with the uniquely generated cumulative inflow curve. Comparing Figure 3.1 and Figure 2.2, Case 1 enables the following observations:

- The outflow curves in both figures are identical, each being generated by the discontinuous inflow rate at $t = 0$. Figure 2.2, Case 1 occurs if the inflow rate is sufficiently large,

Social Optimum for $\alpha_2 = 1$

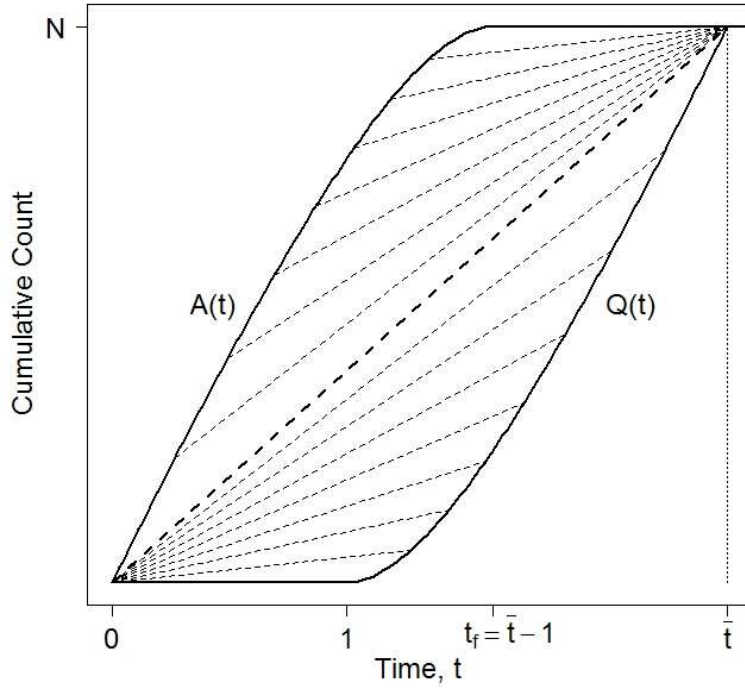


Figure 3.1: $Q(t)$ is the cumulative outflow curve of maximal growth. $A(t)$ is a cumulative inflow curve generated from the discontinuity in the outflow rate at \bar{t} . Any other cumulative inflow curve which lies above $A(t)$ generates the same $Q(t)$; however, the $A(t)$ shown is the only cumulative inflow curve for which no shock waves are present in the system, and thus the traffic dynamics of the system are symmetric in the sense that we can equivalently view the time reversal of the outflow rate as generating the inflow rate. Furthermore, the $A(t)$ shown is the SO solution in the case when $\alpha_2 = 1$, i.e., the $A(t)$ shown minimizes the sum of the area between $A(t)$ and $Q(t)$ plus the area under $Q(t)$, from $t = 0$ to $t = \bar{t}$.

$q_c \geq 1 - \frac{1}{\left(1 + N + \sqrt{N + \left(\frac{N}{2}\right)^2}\right)^2}$, which is precisely the slope at $t = 0$ of the cumulative inflow curve in Figure 3.1. As indicated in the last paragraph of Section 2 in Newell, any cumulative inflow curve lying above the cumulative inflow curve in Figure 3.1 generates the same cumulative outflow curve, being the cumulative outflow curve of maximal growth, but with a deceleration shock wave forming at some x , $0 \leq x \leq 1$. For the cumulative inflow curve in Figure 2.2, Case 1, a shock forms at $(x, t) = (0, t_f)$, and the shock wave path corresponds to the trajectory of the final vehicle departure. For the cumulative inflow curve in Figure 3.1, the shock forms at spacetime point $(x, t) = (1, \bar{t})$

(indicated in Figure 3.1 by the converging dashed lines), the final departure travels at free-flow velocity, and a shock does not occur on its trajectory.

- If shocks are not present for all t and $0 < x < 1$, then (2.2.1) will be strictly satisfied. As indicated in Section 2 of Newell, since (2.2.1) is invariant to changing (x, t) to $(1-x, \bar{t}-t)$, if shocks are not present then there is a one-to-one correspondence between the inflow rate, $a(t)$, and the time reversal of the outflow rate, $q(\bar{t}-t)$. Intuitively, in a system with no shocks we can equivalently consider the time reversal of the outflow rate as generating the inflow rate.
- If the unit travel time cost equals the unit schedule delay cost ($\alpha_2 = 1$ in scaled units), then the SO solution minimizes the sum of the area under the cumulative outflow curve and the area between the cumulative inflow and outflow curves. Section 3 of Newell proves that this area is minimized if the cumulative inflow curve is given as in Figure 3.1. Thus, this cumulative inflow curve is also the SO solution for $\alpha_2 = 1$.

3.2 Inflow and Outflow Rates

If $\alpha_2 < 1$, then minimizing the total trip cost is equivalent to minimizing the sum of the area between the cumulative inflow and outflow curves, plus α_2 multiplied by the area under the cumulative outflow curve. Newell reduces this minimization problem to a calculus of variation problem for the optimal cumulative outflow curve, which he solves in his Appendix, resulting in (3.2) of his paper which we restate in our scaled units:

$$\begin{aligned} Q(t') &= Q(t_0) + \frac{1}{\alpha_2} [Q^*(w_0 + \alpha_2(t' - t'_0)) - Q^*(w_0)] \\ &= \frac{1}{\alpha_2} Q^*(1 + \alpha_2(t' - 1)), \end{aligned}$$

Here Q^* is the same nondimensional cumulative outflow curve of maximal growth from the previous section. Using the functional form in (3.1.1) determined from Greenshields'

Relation, we determine the optimal cumulative outflow curve, $Q(t)$, take its derivative to determine the corresponding outflow rate, $q(t)$, and solve the relation $Q(\bar{t}) = N$ to determine the length of the rush-hour in the corridor, \bar{t} . These results are provided in Table 2.

Inserting these outflow relationships into (2.2.4) determines the corresponding cumulative inflow curve, where $v(q)$ and $w(q)$ are determined via Greenshields' Relation, (A-1) and (2.2.2), respectively. Combining (2.2.2) and $q(t)$ from Table 2 yields

$$w(q) = \frac{1}{\sqrt{1-q(t')}} = 1 + \alpha_2(t' - 1), \quad 1 \leq t' \leq \bar{t}. \quad (3.2.1)$$

Inserting this relation into (2.2.4a) yields

$$t = (1 - \alpha_2)(t' - 1), \quad 1 \leq t' \leq \bar{t} \Leftrightarrow 0 \leq t \leq (1 - \alpha_2)(\bar{t} - 1), \quad (3.2.2)$$

from which we can rewrite w in terms of t :

$$w(q(t)) = 1 + \frac{\alpha_2 t}{1 - \alpha_2}, \quad 0 \leq t \leq (1 - \alpha_2)(\bar{t} - 1). \quad (3.2.3)$$

To determine the cumulative inflow curve up to time $t = (1 - \alpha_2)(\bar{t} - 1)$, insert (3.2.1) into $Q(t)$ from Table 2 to write $Q(t')$ in terms of w , use this expression in (2.2.4b) to write $A(t)$ in terms of w , and finally use (3.2.3) to determine $A(t)$:

$$\begin{aligned} A(t) &= \frac{1}{\alpha_2} \left[w + \frac{1}{w} - 2 \right] - \left(1 - \frac{1}{w^2} \right) \left[w - \frac{2}{1 + \frac{1}{w}} \right] \\ &= \left(\frac{1}{\alpha_2} - 1 \right) \left[w + \frac{1}{w} - 2 \right] \\ &= \frac{t^2}{t + \frac{1}{\alpha_2} - 1}, \quad 0 \leq t \leq (1 - \alpha_2)(\bar{t} - 1). \end{aligned}$$

The remaining portion of the cumulative inflow curve from $t = (1 - \alpha_2)(\bar{t} - 1)$ to $t = t_f$ is generated from the discontinuity in the outflow rate at the point (\bar{t}, N) on the cumulative outflow curve, yielding the same expressions as in (3.1.4) and (3.1.5), and yielding the same

conclusion that $t_f = \bar{t} - 1$, since $A(t_f) = N$. We summarize in Table 2, providing the cumulative inflow curve, $A(t)$, along with its derivative, $a(t)$.

In Figure 3.2 we graph the cumulative inflow and outflow curves for the social optimum for $\alpha_2 < 1$. Consider the limiting case as $\alpha_2 \rightarrow 0$, so that the total trip cost is determined entirely by total travel time. From the results in Table 2, as $\alpha_2 \rightarrow 0$, $\bar{t} \rightarrow \infty$ and $a(t) \rightarrow 0$. Thus, as $\alpha_2 \rightarrow 0$ the inflow is spread over an infinitely long departure interval, so that all vehicles travel at free-flow velocity, thereby minimizing total travel time.

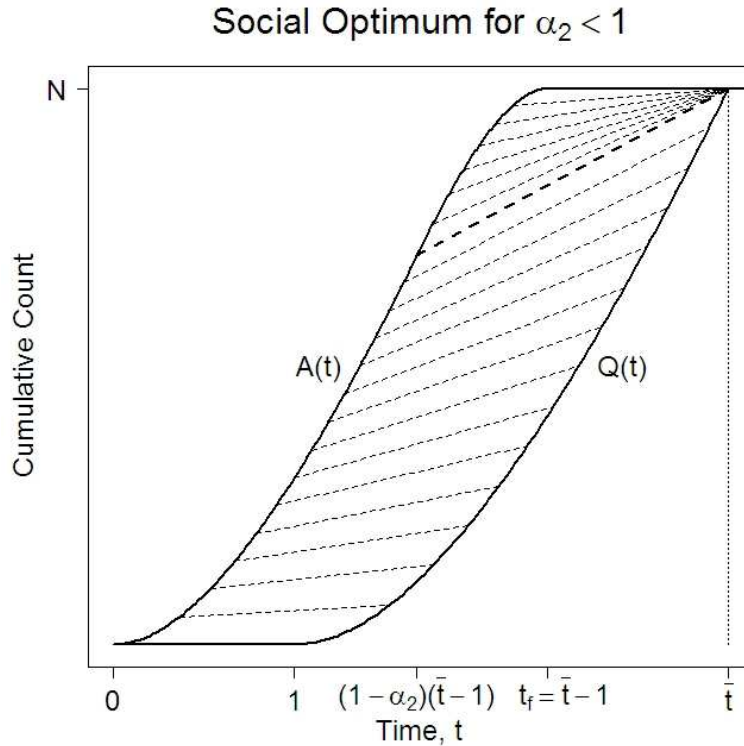


Figure 3.2: Social optimum cumulative inflow and outflow curves for $\alpha_2 < 1$. As α_2 decreases, the area between the inflow and outflow curves (total travel time) decreases, approaching the limiting case in which all vehicles travel at free-flow velocity over an infinitely long rush hour.

3.3 Vehicle Trajectories

Each point, (x, t) , along a vehicle trajectory intersects a characteristic curve with slope w . Under Greenshields' Relation, (A-1) and (2.2.2) determine a differential equation for the trajectory path,

$$\frac{dx}{dt} = \frac{1}{2} \left[1 + \frac{1}{w} \right]. \quad (3.3.1)$$

In Figure 3.3 we graph the characteristic curves in a spacetime diagram for the social optimum, which naturally divide the traffic dynamics into two regions: an upper region consisting of a backwards fan of characteristics, and a lower region. In the upper region the slope of a

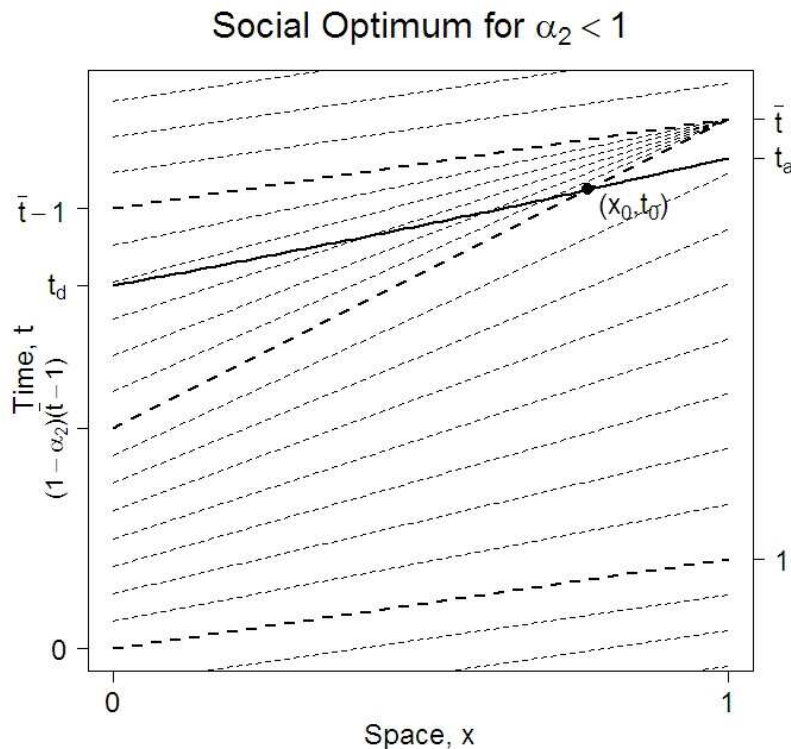


Figure 3.3: Social optimum spacetime diagram. Dashed lines are characteristic lines, which subdivide the traffic dynamics into the two regions indicated with bold dashed lines: an upper region consisting of a backwards fan of characteristics originating from the discontinuity in the flow rate at \bar{t} , and a lower region. We have graphed in bold the trajectory curve of a vehicle that departs at $t_d > (1 - \alpha_2)(\bar{t} - 1)$, traverses the upper region, enters the lower region at point (x_0, t_0) , and arrives at time t_a .

characteristic line through a point (x, t) satisfies

$$w = \frac{\bar{t} - t}{1 - x},$$

and from (3.3.1) a trajectory curve in this region satisfies the differential equation

$$\frac{dx}{dt} = \frac{1}{2} \left[1 + \frac{1 - x}{\bar{t} - t} \right].$$

The general solution to this equation is

$$1 - x = \bar{t} - t + A\sqrt{\bar{t} - t}, \quad (3.3.2)$$

where the arbitrary constant A is determined from the starting point of the trajectory.

In the lower region, by (3.2.3), a characteristic line that originates from $(0, t_0)$ has slope $w = 1 + \frac{\alpha_2 t_0}{1 - \alpha_2}$. If the characteristic line passes through the spacetime point (x, t) , then

$$\frac{t - t_0}{x} = 1 + \frac{\alpha_2 t_0}{1 - \alpha_2},$$

from which we can solve for t_0 , and thus express the slope of the characteristic in terms of x and t as

$$w = 1 + \frac{t - x}{x + \frac{1}{\alpha_2} - 1}.$$

Inserting this expression into (3.3.1) yields the differential equation that is satisfied by trajectory curves in the lower region,

$$\frac{dx}{dt} = \frac{1}{2} \left[1 + \frac{x + \frac{1}{\alpha_2} - 1}{t + \frac{1}{\alpha_2} - 1} \right],$$

whose general solution is

$$x = t + A\sqrt{t + \frac{1}{\alpha_2} - 1}, \quad (3.3.3)$$

where the arbitrary constant A is determined by the trajectory starting point.

For a departure at time $t_d \leq (1 - \alpha_2)(\bar{t} - 1)$, the trajectory is specified in (3.3.3), where the arbitrary constant is chosen so that the trajectory originates from $(0, t_d)$. For a departure at time $t_d > (1 - \alpha_2)(\bar{t} - 1)$, the trajectory is specified in (3.3.2) until it enters the lower region at some point (x_0, t_0) (see Figure 3.3), at which point the trajectory is specified in (3.3.3). We summarize in Table 2, providing explicit expressions for the vehicle trajectories and their arrival times in terms of their departure times, t_d .

3.4 Trip Costs

For a departure at time t_d and arrival at time t_a , travel time is $t_a - t_d$, schedule delay is $\bar{t} - t_a$, and trip cost is $C = t_a - t_d + \alpha_2(\bar{t} - t_a)$. Clearly, schedule delay is a decreasing function of departure time. However, travel time is not an increasing function of departure time, since both the first and last departures travel at free flow velocity. In Figure 3.4 we graph schedule delay cost, travel time cost and trip cost as functions of departure time. For any choice of N and α_2 , the graph of these costs has the same qualitative features.

Using the expressions for $A(t)$, $Q(t)$ and \bar{t} from Table 2, the area under the cumulative outflow curve and between the cumulative inflow and outflow curves can be calculated, and hence the total schedule delay, total travel time and total trip cost can be determined, from (2.4.2), (2.4.3) and (2.4.4), respectively. The results are provided in Table 2.

3.5 Reduction to Bottleneck Model

The bottleneck model (Arnott, de Palma and Lindsey (1990)) is the special case of the Single Entry Corridor Problem with $l = 0$, so that travel time costs are incurred only from time spent in a queue. Arnott, de Palma and Lindsey (1990) provides a heuristic derivation of the social optimum, concluding that the departure rate, with no late arrivals, is capacity flow and that the total travel time cost is $\frac{\alpha_2}{2} \frac{N^2}{q_m}$. We now show how our results for the social optimum with $l = 0$ reduce to these results.

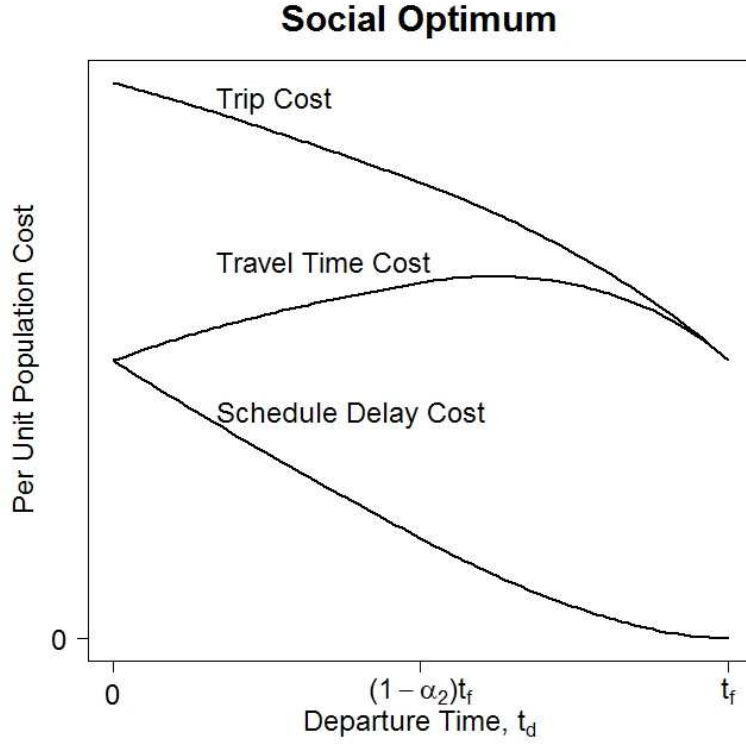


Figure 3.4: Travel time cost, schedule delay cost and trip cost as functions of departure time for the social optimum, with $N = 1$ and $\alpha_2 = 0.5$.

In unscaled units, the expressions for \bar{t} , t_f , $q(t)$ and TTC from Table 2 become:

$$\bar{t} = \frac{l}{v_0} + \frac{N}{2q_m} + \sqrt{\frac{\alpha_1}{\alpha_2} \frac{l}{v_0} \frac{N}{q_m} + \left(\frac{N}{2q_m}\right)^2}$$

$$t_f = \bar{t} - \frac{l}{v_0}$$

$$q(t) = \begin{cases} q_m \left(1 - \frac{1}{\left[1 + \frac{\alpha_2}{\alpha_1} \left(\frac{v_0}{l} t - 1\right)\right]^2} \right) & \frac{l}{v_0} \leq t \leq \bar{t} \\ 0 & \text{otherwise} \end{cases}$$

$$TTC = \alpha_1 q_m \left[\frac{N}{q_m} \left(\frac{l}{v_0} + \frac{\alpha_2}{\alpha_1} t_f \right) - \frac{1}{2} \frac{\alpha_2}{\alpha_1} t_f^2 + \frac{l}{v_0} t_f - \left(\frac{l}{v_0} \right)^2 \frac{\alpha_1}{\alpha_2} \log \left(1 + \frac{\alpha_2 v_0}{\alpha_1 l} t_f \right) \right].$$

Taking the limit as $l \rightarrow 0$ yields $\bar{t} = \frac{N}{q_m}$ and $q(t) = q_m$ for $0 \leq t \leq \bar{t}$, so that the departure rate is capacity flow, as in the bottleneck model. As $l \rightarrow 0$, $t_f = \frac{N}{q_m}$ and, using the fact that $\lim_{x \rightarrow 0} x^2 \log\left(1 + \frac{1}{x}\right) = 0$, total trip cost reduces to $TTC = \frac{\alpha_2 N^2}{2 q_m}$, as in the bottleneck model.

4 User Optimum

Given population, N , and unit schedule delay cost, α_2 , the user optimum, or no-toll equilibrium, is an inflow rate, $a(t)$, such that no individual has an incentive to change their departure time. This condition can be achieved by imposing the *trip-timing (TT) condition* that no vehicle can experience a lower trip cost by departing at a different time. A simple consequence of the TT-condition is that trip cost must be identical for all departure times, t_d .

Let t_d, t'_d denote the departure times of two vehicles that arrive at times t_a, t'_a , respectively. Since their trip costs must be equal,

$$t_a - t_d + \alpha_2 (\bar{t} - t_a) = t'_a - t'_d + \alpha_2 (\bar{t} - t'_a).$$

Assume $t_d < t'_d$, so $t_a < t'_a$, and let $\Delta t_d = t'_d - t_d$ and $\Delta t_a = t'_a - t_a$. The above equation can be rewritten as

$$\Delta t_a = \frac{1}{1 - \alpha_2} \Delta t_d. \tag{4.0.1}$$

Since $\Delta t_a, \Delta t_d > 0$, from (4.0.1) we conclude the TT-condition can be satisfied only if $\alpha_2 < 1$. Section 4 of Newell argues that, for an arbitrary arrival-demand curve, this is a necessary condition for constructing a user optimum. For the specific arrival-demand function for the Single-Entry Corridor Problem with no late arrivals, the previous argument yields the same result.

Since the first departure at time $t = 0$ arrives at time $t = 1$, (4.0.1) implies that a

Time of Last Vehicle Arrival	$\bar{t} = 1 + \frac{N}{2} + \sqrt{\frac{1}{\alpha_2}N + \left(\frac{N}{2}\right)^2}$
Time of Last Vehicle Departure	$t_f = \bar{t} - 1$
Inflow Rate	$a(t) = \begin{cases} \frac{t \left[t + 2 \left(\frac{1}{\alpha_2} - 1 \right) \right]}{\left[t + \frac{1}{\alpha_2} - 1 \right]^2}, & 0 < t < (1 - \alpha_2)(\bar{t} - 1) \\ 1 - \frac{1}{(\bar{t} - t)^2}, & (1 - \alpha_2)(\bar{t} - 1) \leq t < t_f \\ 0, & \text{otherwise} \end{cases}$
Cumulative Inflow Rate	$A(t) = \begin{cases} 0, & t \leq 0 \\ \frac{t^2}{t + \frac{1}{\alpha_2} - 1}, & 0 < t \leq (1 - \alpha_2)(\bar{t} - 1) \\ N - (\bar{t} - t + \frac{1}{\bar{t} - t} - 2), & (1 - \alpha_2)(\bar{t} - 1) < t \leq t_f \\ N, & t > t_f \end{cases}$
Outflow Rate	$q(t) = \begin{cases} 1 - \frac{1}{[1 + \alpha_2(t-1)]^2}, & 1 \leq t \leq \bar{t} \\ 0, & \text{otherwise} \end{cases}$
Cumulative Outflow Rate	$Q(t) = \begin{cases} 0, & t \leq 1 \\ \frac{1}{\alpha_2} \left[1 + \alpha_2(t-1) + \frac{1}{1 + \alpha_2(t-1)} - 2 \right], & 1 < t \leq \bar{t} \\ N, & t > \bar{t} \end{cases}$
Arrival Time if $0 \leq t_d \leq (1 - \alpha_2)(\bar{t} - 1)$	$t_a = 1 + \frac{1}{2} \left(\frac{t_d^2}{t_d + \frac{1}{\alpha_2} - 1} \right) + \sqrt{\frac{1}{\alpha_2} \left(\frac{t_d^2}{t_d + \frac{1}{\alpha_2} - 1} \right) + \frac{1}{4} \left(\frac{t_d^2}{t_d + \frac{1}{\alpha_2} - 1} \right)^2}$
Vehicle Trajectory if $0 \leq t_d \leq (1 - \alpha_2)(\bar{t} - 1)$	$x(t) = t - t_d \sqrt{\frac{t + \frac{1}{\alpha_2} - 1}{t_d + \frac{1}{\alpha_2} - 1}}$
Spacetime Point where Vehicle Trajectory Enters Lower Region of Characteristics if $(1 - \alpha_2)(\bar{t} - 1) < t_d \leq \bar{t} - 1$	$(x_0, t_0) = \left(1 - \frac{\alpha_2(\bar{t}-1)+1}{(\alpha_2(\bar{t}-1))^2} \frac{(\bar{t}-1-t_d)^2}{\bar{t}-t_d}, \bar{t} - \left(1 + \frac{1}{\alpha_1(\bar{t}-1)} \right)^2 \frac{(\bar{t}-1-t_d)^2}{\bar{t}-t_d} \right)$
Arrival Time if $(1 - \alpha_2)(\bar{t} - 1) < t_d \leq \bar{t} - 1$	$t_a = 1 + \frac{1}{2} \left[\frac{(t_0 - x_0)^2}{t_0 + \frac{1}{\alpha_2} - 1} \right] + \sqrt{\frac{1}{\alpha_2} \left[\frac{(t_0 - x_0)^2}{t_0 + \frac{1}{\alpha_2} - 1} \right] + \frac{1}{4} \left[\frac{(t_0 - x_0)^2}{t_0 + \frac{1}{\alpha_2} - 1} \right]^2}$
Vehicle Trajectory if $(1 - \alpha_2)(\bar{t} - 1) < t_d \leq \bar{t} - 1$	$x = \begin{cases} 1 - (\bar{t} - t) + (\bar{t} - 1 - t_d) \sqrt{\frac{\bar{t} - t}{\bar{t} - t_d}}, & t_d \leq t \leq t_0 \\ t - (t_0 - x_0) \sqrt{\frac{t + \frac{1}{\alpha_2} - 1}{t_0 + \frac{1}{\alpha_2} - 1}}, & t_0 < t \leq t_a \end{cases}$
Total Schedule Delay	$TSD = \frac{1}{2}t_f^2 - \frac{1}{\alpha_2}t_f + \frac{1}{\alpha_2^2} \log(1 + \alpha_2 t_f)$
Total Travel Time	$TTT = N(1 + \alpha_2 t_f) - \alpha_2 t_f^2 + 2t_f - \frac{2}{\alpha_2} \log(1 + \alpha_2 t_f)$
Total Trip Cost	$TTC = N(1 + \alpha_2 t_f) - \frac{1}{2}\alpha_2 t_f^2 + t_f - \frac{1}{\alpha_2} \log(1 + \alpha_2 t_f)$

Table 2: Table of results for the social optimum (scaled units).

departure at time $t = t_d$ satisfies

$$t_a = 1 + \frac{1}{1 - \alpha_2} t_d. \quad (4.0.2)$$

Since cumulative flow is constant along a trajectory,

$$\int_0^{t_d} a(t) dt = \int_1^{t_a} q(t) dt,$$

and differentiating with respect to t_d yields

$$a(t_d) = \frac{1}{1 - \alpha_2} q(t_a). \quad (4.0.3)$$

Thus, along a vehicle trajectory, from the corridor entry-point to the CBD the flow rate decreases by the multiplicative factor $\frac{1}{1 - \alpha_2}$.

4.1 Qualitative Features

In the following lemmas we show that a consequence of (4.0.3) is that $a(0) = 0$ and that $a(t)$ is a continuously increasing function from time $t = 0$ up to the final departure at time $t = t_f$, at which time $a(t)$ discontinuously decreases to zero.

Lemma 4.1.1. *The corridor inflow and outflow rates discontinuously decrease to zero at times t_f and \bar{t} , respectively.*

Proof. Since schedule delay is a decreasing function of departure time, and since trip cost is constant, travel time must be an increasing function of departure time. As a consequence, the final departure does not travel at free-flow velocity; thus, its trajectory coincides with a shock wave path (see Section 2.2.2). \square

Lemma 4.1.2. *The corridor inflow rate, $a(t)$, must be an increasing function of departure time from $t = 0$ to the final departure at time $t = t_f$.*

Proof. We use proof by contradiction. Since the first departure occurs at $t = 0$, $a(t) = 0$ for $t < 0$. Denote the first time for which $a(t)$ is nonincreasing by t_{d_1} , and let t_{a_1} denote the arrival time of a vehicle that departs at time t_{d_1} . The outflow rate at t_{a_1} is determined by characteristic lines that originate from $x = 0$ at times earlier than t_{d_1} ; thus, the outflow rate must be increasing at time t_{a_1} . However, by (4.0.3), since the inflow rate is nonincreasing at t_{d_1} , the outflow rate is also nonincreasing at t_{a_1} , which is a contradiction. \square

Lemma 4.1.2 implies that, except for the trajectory of the last departure, shocks do not occur in the UO solution.

Lemma 4.1.3. *The corridor inflow rate, $a(t)$, does not discontinuously increase.*

Proof. By Lemma 4.1.2, since $a(t)$ is increasing, the outflow rate, $q(t)$, is also increasing. If $a(t)$ discontinuously increased, then $q(t)$ would be obtained from a rarefaction fan of characteristic waves, so $q(t)$ would increase continuously. Thus, $q(t)$ increases continuously, whether or not $a(t)$ has a discontinuous increase. From (4.0.3), the continuity of $q(t)$ implies the continuity of $a(t)$. \square

In particular, since $a(t) = 0$ for $t < 0$, Lemma 4.1.3 implies that $a(0) = 0$.

4.2 Inflow and Outflow Curves

For the following discussion, refer to Figure 4.1. A departure at time t_d arrives at the CBD at time t_a . Using (2.2.4) we can draw a line of constant flow from $(t_a, Q(t_a))$ to a point $(t_0, A(t_0))$, where $a(t_0) = q(t_a)$. (2.2.4a) yields t_0 in terms of t_a as

$$t_0 = t_a - \frac{1}{\sqrt{1 - q(t_a)}},$$

which can be rewritten in terms of t_d using (4.0.2) and (4.0.3)

$$t_0 = \frac{1}{1 - \alpha_2} t_d - \left(\frac{1}{\sqrt{1 - (1 - \alpha_2)a(t_d)}} - 1 \right). \quad (4.2.1)$$

UO: Cumulative Flow Curves

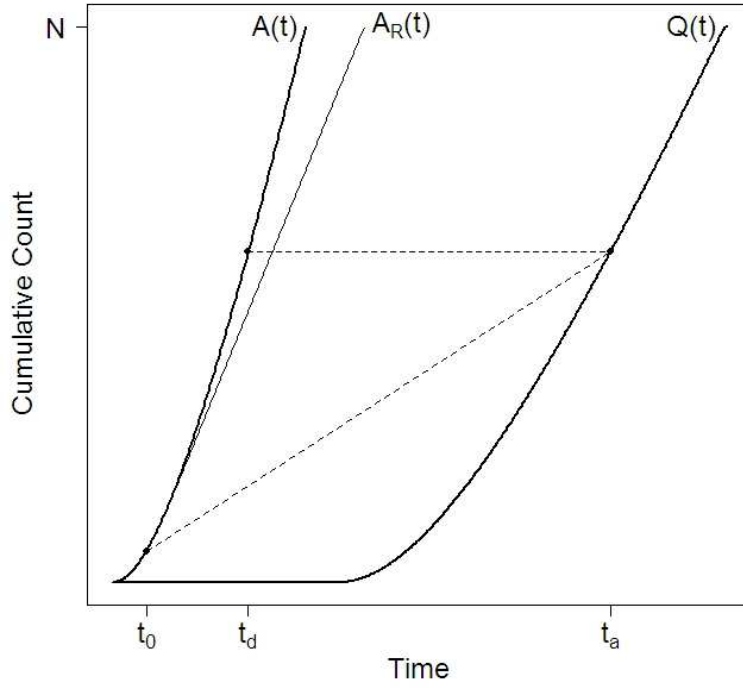


Figure 4.1: Cumulative corridor inflow, road inflow, and corridor outflow curves, $A(t)$, $A_R(t)$, and $Q(t)$, respectively. The slope of $A_R(t)$ cannot exceed capacity flow. The horizontal distance between $A(t)$ and $A_R(t)$ is time spent in a queue. A departure at time t_d arrives at the CBD at time t_a , indicated by the horizontal dashed line. The diagonal dashed line is a line of constant flow, so the slope of $A(t)$ at t_0 equals the slope of $Q(t)$ at t_a .

Since $a(t_0) = q(t_a)$, (4.0.3) can be rewritten as $a(t_d) = \frac{1}{1-\alpha_2}a(t_0)$, and substituting t_0 with (4.2.1) yields an implicit expression for $a(t_d)$ in terms of t_d :

$$a(t_d) = \frac{1}{1-\alpha_2}a \left(\frac{1}{1-\alpha_2}t_d - \left[\frac{1}{\sqrt{1-(1-\alpha_2)a(t_d)}} - 1 \right] \right). \quad (4.2.2)$$

(4.2.2) is satisfied by the corridor inflow rate, $a(t)$, for all departure times, t_d . If $a(t)$ exceeds capacity flow, then a queue develops since the road inflow rate cannot exceed capacity flow.

We use an iterative procedure⁶ to analytically solve (4.2.2) for $a(t_d)$, $0 < t_d < t_f$. To simplify the notation, we replace t_d with t , denote $\frac{1}{1-\alpha_2}$ by σ , and denote $\frac{1}{\sqrt{1-a(t)}} - 1$ by

⁶The following iterative procedure is based on work in Danqing Hu's Ph.D. dissertation, *Three Essays on Urban and Transport Economics*, Department of Economics, University of Wisconsin-Madison.

$g(a(t))$, so (4.2.2) becomes

$$a(t) = \sigma a \left(\sigma t - g \left(\frac{1}{\sigma} a(t) \right) \right). \quad (4.2.3)$$

In Table 3 we repeatedly iterate (4.2.3) n times, yielding the following n -th iterated expression for $a(t)$:

$$a(t) = \sigma^n a \left(\sigma^n \left[t - \sum_{j=1}^n \frac{1}{\sigma^j} g \left(\frac{1}{\sigma^j} a(t) \right) \right] \right). \quad (4.2.4)$$

From the lemmas of the previous section, $a(t)$ is a continuously increasing function on $0 \leq t < t_f$; thus, its inverse is well-defined on this interval, so (4.2.4) may be rewritten as

$$(1 - \alpha_2)^n a^{-1} [(1 - \alpha_2)^n a(t)] = t - \sum_{j=1}^n (1 - \alpha_2)^j \left[\frac{1}{\sqrt{1 - (1 - \alpha_2)^j a(t)}} - 1 \right].$$

Since $a(0) = 0$, taking the limit as $n \rightarrow \infty$, the left-hand side becomes zero and we obtain an expression for the inverse of the inflow rate, $t = t(a)$,

$$t(a) = \sum_{j=1}^{\infty} (1 - \alpha_2)^j \left[\frac{1}{\sqrt{1 - (1 - \alpha_2)^j a}} - 1 \right], \quad (4.2.5)$$

which is a convergent series for $0 \leq a < \frac{1}{1 - \alpha_2}$. The inflow rate, $a(t)$, increases up to some final value, a_f , at time t_f , when the entire population has departed, i.e., $\int_0^{t_f} a(t) dt = N$, which is equivalent to

$$\int_0^{a_f} t(a) da + N = t_f a_f.$$

Integrating (4.2.5), replacing t_f with $t(a_f)$, and algebraically solving for N yields

$$N = \sum_{j=1}^{\infty} \frac{2 \left[1 - \sqrt{1 - (1 - \alpha_2)^j a_f} \right] - (1 - \alpha_2)^j a_f}{\sqrt{1 - (1 - \alpha_2)^j a_f}}, \quad 0 \leq a_f < \frac{1}{1 - \alpha_2}. \quad (4.2.6)$$

Given a population size, N , (4.2.6) must be numerically solved to determine a_f , which is inserted into (4.2.5) to determine t_f . If $a_f > 1$, then a queue develops at some time, denoted

$$\begin{aligned}
a(t) &= \sigma a \left(\sigma t - g \left(\frac{1}{\sigma} a(t) \right) \right) \\
&= \sigma a(u_1), \text{ where } u_1 = \sigma t - g \left(\frac{1}{\sigma} a(t) \right) \\
\\
a(t) &= \sigma^2 a \left(\sigma u_1 - g \left(\frac{1}{\sigma} a(u_1) \right) \right) \\
&= \sigma^2 a \left(\sigma^2 t - \sigma g \left(\frac{1}{\sigma} a(t) \right) - g \left(\frac{1}{\sigma^2} a(t) \right) \right) \\
&= \sigma^2 a(u_2), \text{ where } u_2 = \sigma^2 t - \sigma g \left(\frac{1}{\sigma} a(t) \right) - g \left(\frac{1}{\sigma^2} a(t) \right) \\
\\
a(t) &= \sigma^3 a \left(\sigma u_2 - g \left(\frac{1}{\sigma} a(u_2) \right) \right) \\
&= \sigma^3 a \left(\sigma^3 t - \sigma^2 g \left(\frac{1}{\sigma} a(t) \right) - \sigma g \left(\frac{1}{\sigma^2} a(t) \right) - g \left(\frac{1}{\sigma^3} a(t) \right) \right) \\
&= \sigma^3 a(u_3), \text{ where } u_3 = \sigma^3 t - \sigma^2 g \left(\frac{1}{\sigma} a(t) \right) - \sigma g \left(\frac{1}{\sigma^2} a(t) \right) - g \left(\frac{1}{\sigma^3} a(t) \right) \\
\\
&\vdots \\
\\
a(t) &= \sigma^n a \left(\sigma^n \left[t - \sum_{j=1}^n \frac{1}{\sigma^j} g \left(\frac{1}{\sigma^j} a(t) \right) \right] \right) \\
&= \sigma^n a(u_n), \text{ where } u_n = \sigma^n \left[t - \sum_{j=1}^n \frac{1}{\sigma^j} g \left(\frac{1}{\sigma^j} a(t) \right) \right]
\end{aligned}$$

Table 3: Repeated iteration of (4.2.3), which yields the n -th iterated expression for $a(t)$.

as t_Q . For a given value of α_2 , if N is sufficiently large then a queue develops. Let us temporarily denote the critical value of N such that a queue develops as N_c , i.e., if $N > N_c$ then a queue develops. From (4.2.6),

$$N_c = \sum_{j=1}^{\infty} \frac{2 \left[1 - \sqrt{1 - (1 - \alpha_2)^j} \right] - (1 - \alpha_2)^j}{\sqrt{1 - (1 - \alpha_2)^j}}. \quad (4.2.7)$$

From (4.2.7) it can easily be shown that N_c is a decreasing function of α_2 which satisfies $\lim_{\alpha_2 \rightarrow 1} N_c = 0$, and $\lim_{\alpha_2 \rightarrow 0} N_c = \infty$.

Using the above procedure one may numerically construct the inflow rate for the UO solution, $a(t)$. Numerically integrating $a(t)$ yields the cumulative inflow rate, $A(t)$, from which we obtain the cumulative outflow rate $Q(t)$ via $Q(t_a) = A(t_d)$, where $t_a = 1 + \frac{1}{1-\alpha_2}t_d$. In Figure 4.2 we graph the numerically obtained cumulative corridor inflow, road inflow and outflow curves for given values $N = 0.8$ and $\alpha_2 = 0.5$. We chose N large enough (relative to α_2) so that a queue develops. The dashed lines are lines of constant flow, and show how the population inflow determines the outflow. In particular, note that the outflow is completely determined by the inflow that occurs before the queue develops, i.e., before capacity inflow is reached. The trajectory of the final departure is a shock wave path of decreasing shock strength.

4.3 Vehicle Trajectories

Given values for the population size, N , and unit schedule delay cost, α_2 , we use the procedure outlined in the previous section to numerically construct the inflow rate. The inflow rate allows us to determine the slope of the characteristic lines in spacetime emanating from the t -axis, from which we numerically determine vehicle trajectory curves. Since we do not have an analytic expression for the inflow rate, $a(t)$, we are not able to analytically construct the differential equation which is satisfied by vehicle trajectory curves.

Recall that, if N is sufficiently large relative to α_2 , then the corridor inflow rate reaches

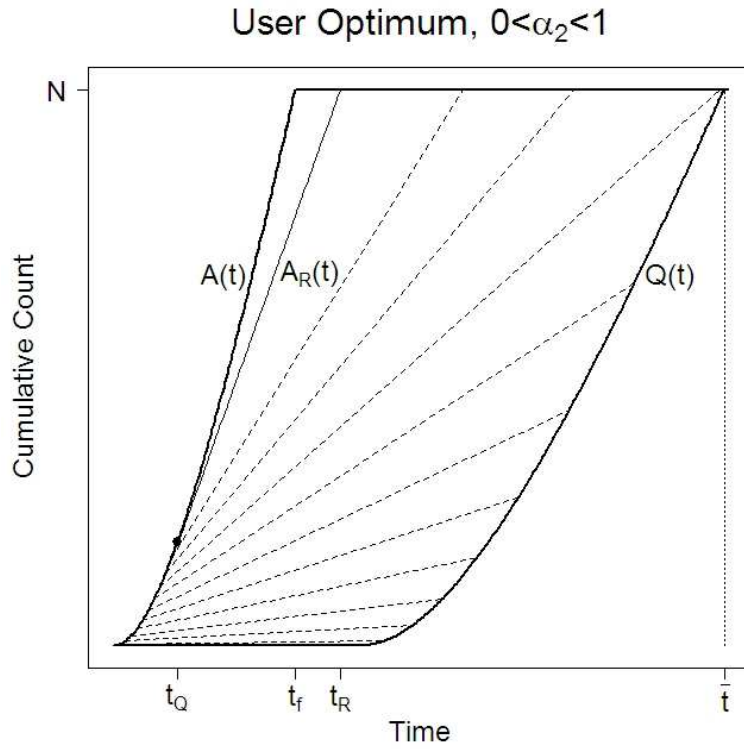


Figure 4.2: Cumulative corridor inflow, road inflow, and corridor outflow curves, $A(t)$, $A_R(t)$, and $Q(t)$, respectively, with $N = 0.8$ and $\alpha_2 = 0.5$. A queue develops at time t_Q , indicated by the solid dot, when the corridor inflow rate reaches capacity flow. As indicated by the dashed lines of constant flow, the outflow is completely determined by the inflow that occurs before the queue develops.

capacity flow at time t_Q , and continues to increase until the final departure at time t_f . The road inflow rate remains at capacity flow from time t_Q until time $t_R > t_f$, where t_R is the time the final vehicle departure enters the road. All departures after t_Q enter a queue before entering the road, and queueing time increases with departure time. In Figure 4.3 we have graphed characteristic lines and vehicle trajectory curves for a user optimum solution in which a queue develops.

User Optimum, $0 < \alpha_2 < 1$

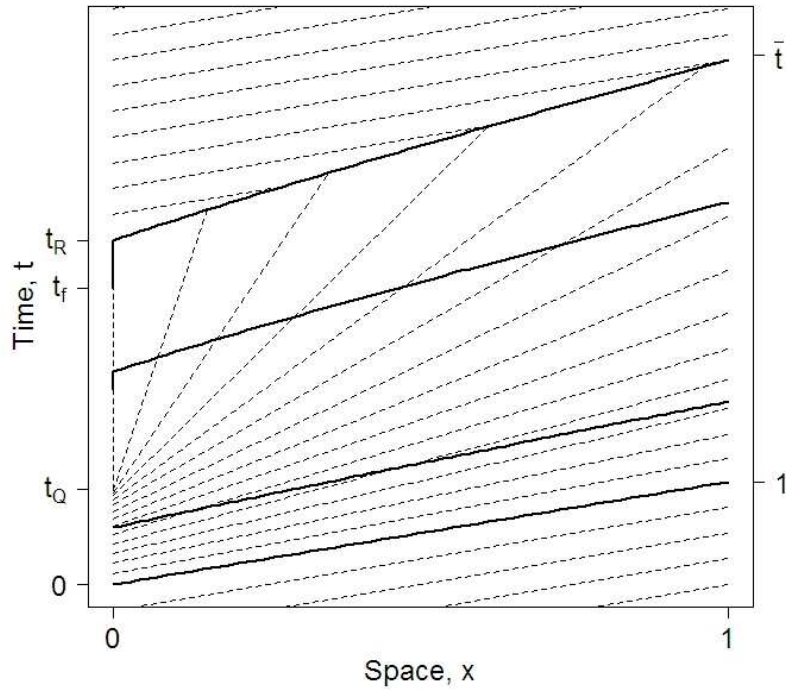


Figure 4.3: Dashed lines are characteristics whose slope depends upon the road inflow rate at the entry point at $x = 0$. For $t_Q < t \leq t_R$ a queue is present and the road inflow rate is capacity flow, so that characteristics are vertical lines. We have plotted four vehicle trajectory curves in bold: The first vehicle departure that travels at free-flow velocity; a departure that occurs before t_Q and does not experience a queue; a departure that occurs after t_Q and experiences a queue; and the final vehicle departure at time t_f that experiences a queue until entering the road at time t_R .

4.4 Trip Costs

From (4.0.2) the travel time for a departure at time t_d is a linear function of t_d ,

$$t_a - t_d = 1 + \frac{\alpha_2}{1 - \alpha_2} t_d.$$

Since trip cost is constant, schedule delay is also a linear function of t_d , summarized in (4.4.1), and graphed in Figure 4.4:

$$\begin{aligned}
 C &= \text{Travel Time} + \alpha_2(\text{Schedule Delay}) \\
 &= 1 + \frac{\alpha_2}{1 - \alpha_2}t_d + \alpha_2 \left(\bar{t} - 1 - \frac{1}{1 - \alpha_2}t_d \right) \\
 &= 1 + \alpha_2(\bar{t} - 1)
 \end{aligned}
 \tag{4.4.1}$$

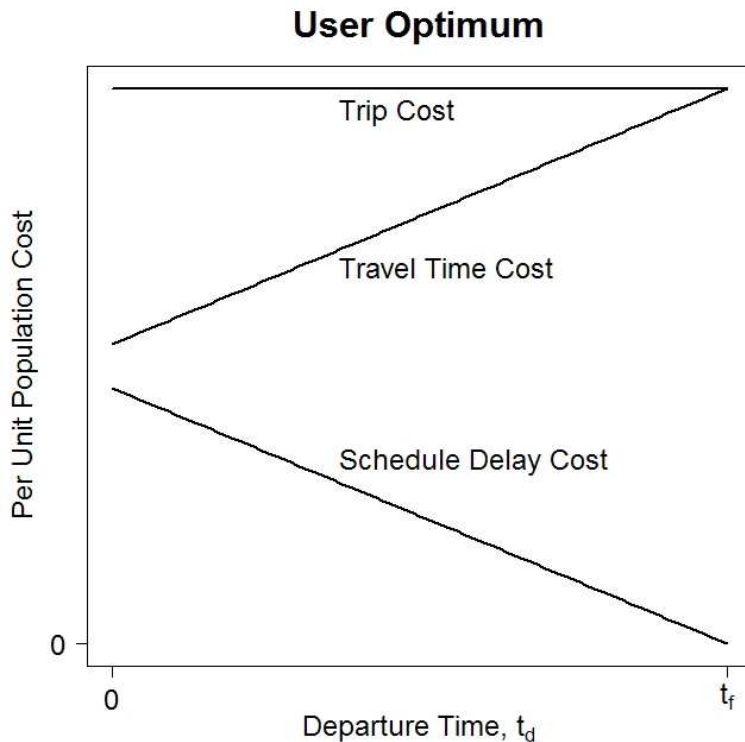


Figure 4.4: Travel time cost, schedule delay cost and trip cost as functions of departure time for the user optimum, with $N = 1$ and $\alpha_2 = 0.5$. The trip-timing condition requires that trip cost is constant and travel time cost is a linear function of departure time, so that schedule delay is also a linear function of departure time.

Since we have not obtained closed-form expressions for the cumulative inflow and outflow curves, we cannot obtain a closed-form expression for the total travel time or schedule delay. However, since the trip cost is constant for all vehicles, we can analytically determine the

total trip cost, in terms of either the final departure time, t_f , or the final arrival time, \bar{t} :

$$\begin{aligned} TTC &= N \left[1 + \frac{\alpha_2}{1 - \alpha_2} t_f \right] \\ &= N [1 + \alpha_2 (\bar{t} - 1)]. \end{aligned} \tag{4.4.2}$$

4.5 Reduction to Bottleneck Model

Arnott, de Palma and Lindsey (1990) show that the user optimum for the bottleneck model with no late arrivals entails a constant inflow rate of $\frac{1}{1 - \frac{\alpha_2}{\alpha_1}} q_m$, with a resulting total trip cost of $\alpha_2 \frac{N^2}{q_m}$. We now show that the UO solution for the Single-Entry Corridor Problem with no late arrivals reduces to the bottleneck model as $l \rightarrow 0$.

Since road inflow cannot exceed capacity flow, the outflow, $q(t)$, cannot exceed capacity flow. Rewriting (4.0.3) in unscaled units, we conclude that corridor inflow cannot exceed $\frac{1}{1 - \frac{\alpha_2}{\alpha_1}} q_m$. In (4.2.5) we provided an expression for the inverse of the inflow rate, which in unscaled units becomes

$$t = \frac{l}{v_0} \sum_{j=1}^{\infty} \left(1 - \frac{\alpha_2}{\alpha_1}\right)^j \left[\frac{1}{\sqrt{1 - \left(1 - \frac{\alpha_2}{\alpha_1}\right)^j \frac{a}{q_m}}} - 1 \right].$$

The infinite sum in this equation converges if $a < \frac{1}{1 - \frac{\alpha_2}{\alpha_1}} q_m$. In the limit as $l \rightarrow 0$, to ensure that the right-hand side of this equation does not equal zero, the infinite sum must diverge. Since (4.0.3) implies $a \leq \frac{1}{1 - \frac{\alpha_2}{\alpha_1}} q_m$, we conclude that as $l \rightarrow 0$, $a(t) = \frac{1}{1 - \frac{\alpha_2}{\alpha_1}} q_m$, reproducing the UO solution for the bottleneck model. Since, in the limit as $l \rightarrow 0$ the inflow rate is constant, the final departure time is

$$t_f = \frac{N}{\frac{1}{1 - \frac{\alpha_2}{\alpha_1}} q_m}.$$

Rewriting the expression for the total trip cost, (4.4.2), in unscaled units yields

$$TTC = N \left[\alpha_1 \frac{l}{v_0} + \frac{\alpha_2}{1 - \frac{\alpha_2}{\alpha_1}} t_f \right],$$

and taking the limit as $l \rightarrow 0$ we obtain $TTC = \alpha_2 \frac{N^2}{q_m}$, as in the bottleneck model.

5 Economic Properties

This section provides a brief discussion of some economic properties of the SO and UO of the single-entry corridor problem. In particular, it will examine: i) the properties of the cost functions for the SO and UO (the supply side of the transportation market); ii) the properties of the time-varying toll that decentralizes the social optimum; and iii) how these properties differ from the corresponding properties of the bottleneck model.

5.1 The SO Cost Function

The total trip cost function relates total trip cost to the number of users. The total variable trip cost equals total trip cost minus the cost that would be incurred were there no congestion, which is the cost of users' free-flow travel time. There are two components of total variable trip cost, total schedule delay cost and total variable travel time cost. We employ standard notation with respect to costs. As prefixes to symbols, T denotes total, A average, M marginal, F fixed, and V variable, and as a suffix C denotes cost. The core of a symbol indicates the nature of the quantity or cost. Thus, for example, TTC denotes total trip cost, while $MVTC$ denotes marginal variable trip cost.

To simplify the algebra, we retain the normalization from the earlier sections of the paper. Length units are chosen such that the length of the road equals 1.0, time units such that the free-flow travel time on the road equals 1.0, population units such that $N = 1.0$ corresponds to the road's capacity flow per unit time, and cost units such that the value of travel time

equals 1.0

Table 4 records the relevant algebraic results for the social optimum. All results are presented in normalized form, and are obtained straightforwardly from previous results. Row 1 records the algebra for schedule delay cost, row 2 for variable travel time cost (travel time in excess of free flow travel time), and row 3 for variable trip cost (the sum of schedule delay and variable travel time cost). Column 1 gives the expression for total cost (e.g., total schedule delay cost), column 2 for marginal cost, column 3 for private cost, and column 4 for externality cost, which equals the difference between marginal cost and private cost. Note that the marginal costs are independent of departure time but that the private costs and the externality costs depend on departure time.

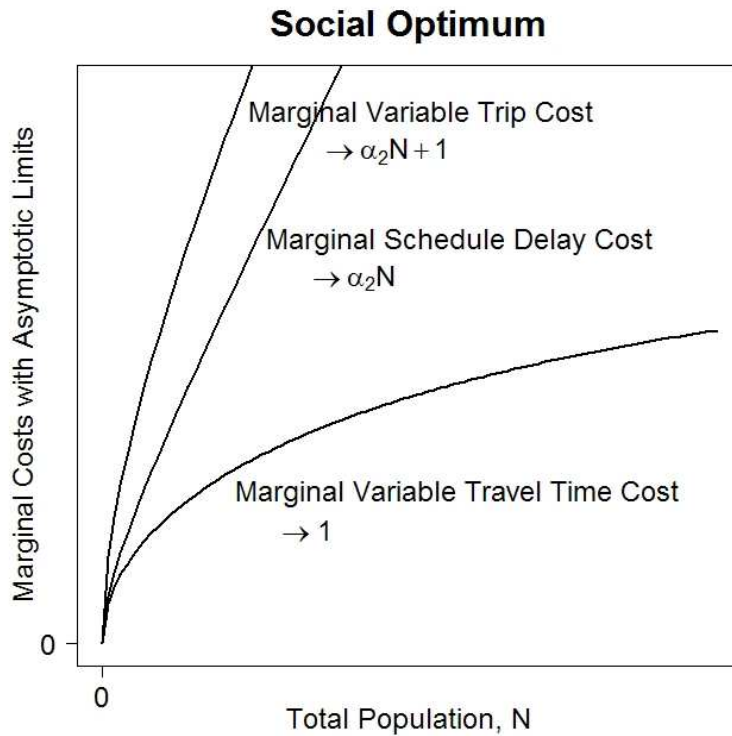


Figure 5.1: Marginal costs as functions of population for the social optimum, with $\alpha_2 = 0.5$.

Figure 5.1 plots marginal variable travel time cost, marginal schedule delay cost, and marginal variable trip cost for the social optimum, as functions of population, and records

	Total Cost
Schedule Delay	$\frac{1}{2}\alpha_2 t_f^2 - t_f + \frac{1}{\alpha_2} \log(1 + \alpha_2 t_f)$
Variable Travel Time	$N\alpha_2 t_f - \alpha_2 t_f^2 + 2t_f - \frac{2}{\alpha_2} \log(1 + \alpha_2 t_f)$
Variable Trip	$N\alpha_2 t_f - \frac{1}{2}\alpha_2 t_f^2 + t_f - \frac{1}{\alpha_2} \log(1 + \alpha_2 t_f)$

	Marginal Cost	Private Cost	Externality Cost
Schedule Delay	$\frac{N(1+\alpha_2 t_f)}{2t_f - N}$	$\alpha_2(\bar{t} - t_a)$	$\frac{N(1+\alpha_2 t_f)}{2t_f - N} - \alpha_2(\bar{t} - t_a)$
Variable Travel Time	$\frac{N}{2t_f - N}$	$t_a - t_d - 1$	$\frac{N}{2t_f - N} - (t_a - t_d - 1)$
Variable Trip	$\alpha_2 t_f$	$\alpha_2(\bar{t} - t_a) + t_a - t_d - 1$	$t_d - (1 - \alpha_2)(t_a - 1)$

Table 4: Normalized Cost Formulae: Social Optimum ($\bar{t} = t_f + 1$ and $t_f = \frac{N}{2} + \sqrt{\frac{N}{\alpha_2} + \left(\frac{N}{2}\right)^2}$).

the asymptotic value of each marginal cost as N approaches infinity. Consider first marginal variable travel time cost. In the limit as N approaches zero, vehicles travel at free-flow travel speed, and both private and marginal variable travel time costs are zero. As N increases, mean travel time increases, until in the limit marginal variable travel time cost equals 1.0, which with Greenshields' Relation is the variable travel time cost when traveling the entire length of the road at capacity flow. Consider next marginal schedule delay cost. In the limit as N approaches zero, marginal schedule delay cost is of order $N^{\frac{1}{2}}$ and so approaches zero. In the limit as N approaches infinity, marginal schedule delay cost equals⁷ $\alpha_2 t_f - 1 = \alpha_2 N$.

Since the social optimum entails the minimization of total variable trip costs, the Envelope Theorem can be applied to compute marginal variable trip cost. In particular, it can be computed as the variable trip cost of a vehicle added just before the first vehicle to depart, holding fixed the departure pattern of all other vehicles. This vehicle travels at free-flow travel speed, does not affect the traffic flow of later vehicles, and incurs a schedule delay of t_f . Thus, marginal variable trip cost equals $\alpha_2 t_f$. From the expression for t_f given in Table 4, it follows that the elasticity of marginal variable trip cost with respect to N , $E_{MVT C:N}$, increases monotonically in N , rising from 0.5 when N is zero to 1.0 when N is infinite.

An important implication of this result is that at the social optimum the average externality cost imposed by a vehicle on other vehicles is strictly less than the average variable trip cost. Put alternatively, on average, the externality cost a vehicle imposes on other vehicles is less than the increase in cost it experiences due to congestion. In contrast, in the bottleneck model, on average, the externality cost a vehicle imposes on other vehicles equals the increase in cost it experiences due to congestion, while in the conventional static model the externality cost a vehicle imposes on other vehicles is several times the increase in cost it experiences due to congestion.

⁷Note that one cannot apply the Envelope Theorem to derive the marginal variable travel time cost and marginal schedule delay cost. The addition of a vehicle alters the time pattern of inflows and outflows of inframarginal drivers, and these adjustments do not net out.

5.2 The First-Best, Time-Varying Toll

Economists use the term first best to refer to a situation where the only constraints the policy maker/social planner faces are technological and resource constraints, as is the case in this paper. The first-best, time-varying toll decentralizes the social optimum; that is, imposition of this toll results in a user optimum allocation that coincides with the social optimum allocation. This occurs when each vehicle faces the social costs of its actions, and is achieved by imposing a toll at each point in time equal to the externality cost imposed by the vehicle, evaluated at the social optimum. The externality cost in turn equals the difference between the marginal variable trip cost and the private variable trip cost (the variable travel time cost incurred by a vehicle, $t_a - t_d - 1$, plus the schedule delay cost it incurs, $\alpha_2(\bar{t} - t_a)$). Thus, as a function of departure time, the first-best time-varying toll equals

$$\tau(t_d) = \alpha_2 t_f - [\alpha_2(\bar{t} - t_a(t_d)) + (t_a(t_d) - t_d - 1)]. \quad (5.2.1)$$

The expression for t_f is given in Table 4, and the form of the function $t_a(t_d)$, which relates arrival time to departure time, is given in Table 2.

Figure 5.2 plots marginal variable trip cost, private variable trip cost, and the decentralizing toll, as functions of departure time with $\alpha_2 = 0.5$ and $N = 1$. The toll equals zero for the first vehicle to depart since that vehicle imposes no externality cost on other vehicles, experiencing the entire marginal variable trip cost as its private schedule delay cost. The toll increases at an increasing rate over the morning rush hour. The last vehicle experiences no schedule delay cost and no variable travel time cost, so that its externality cost equals the entire marginal variable trip cost.

Results on first-best optimal capacity with inelastic demand can be obtained straightforwardly. First-best optimal capacity minimizes the total cost associated with transporting the N vehicles from the origin to the destination, including the cost of constructing the road. The self-financing results carry through. Since the congestion technology has the property

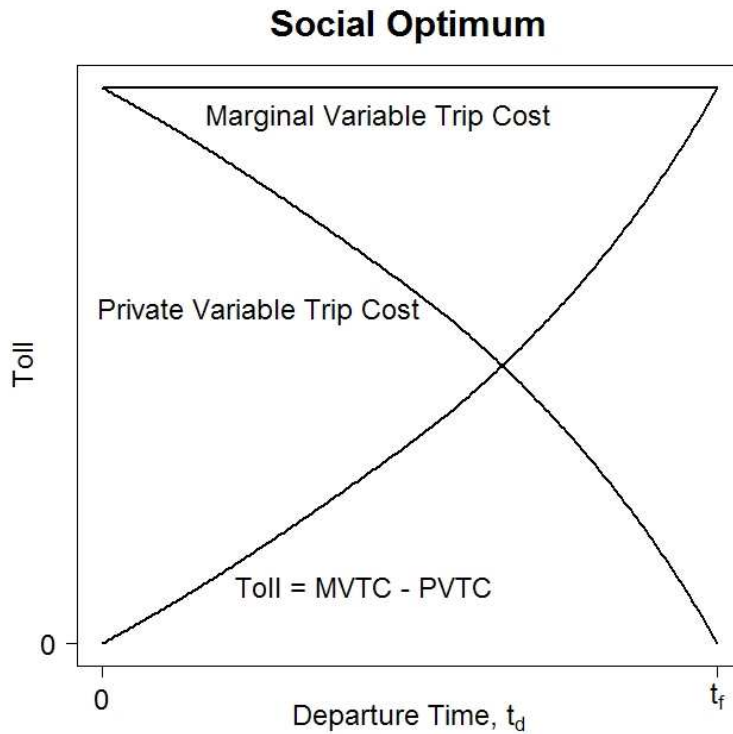


Figure 5.2: Marginal and private variable trip costs, and the toll, as functions of departure time for the social optimum, with $N = 1$ and $\alpha_2 = 0.5$.

that velocity depends on density per unit area, the average trip cost function is homogeneous of degree zero in the volume/capacity ratio, where here volume is population. From familiar statements of the Self-Financing Theorem, it follows that the revenue from the optimal toll covers the cost of constructing optimal capacity if there are constant costs to capacity expansion.

5.3 User Optimum/No-Toll Equilibrium

Since the user optimum does not admit a neat analytical solution, we proceed using heuristic argument. We continue to apply the normalizations employed in the previous sections, so that solutions differ according to only two parameters, N and α_2 .

The first person to depart experiences zero variable travel time. If it were otherwise, a person departing infinitesimally earlier would experience a lower trip cost, which is incon-

sistent with equilibrium. Consistency with the trip-timing equilibrium condition requires as well that travel time, as a function of departure time, increase as the rate $\frac{\alpha_2}{1-\alpha_2}$. These two results imply that the departure rate function (with $t = 0$ denoting the time of the first departure) is independent of N . Extra vehicles are accommodated through a lengthening of the rush hour, with the entry rate of these vehicles being determined by the trip-timing condition. Thus, a vehicle imposes a schedule delay externality on those vehicles that depart earlier and a travel time externality on those vehicles that depart later. The common trip price, in excess of free-flow travel time costs, $p(N)$, equals the schedule delay cost of the first person to depart and also the variable travel time cost of the last person to depart:

$$p(N) = \alpha_2 (\bar{t}(N) - 1) = \bar{t}(N) - t_f(N) - 1. \quad (5.3.1)$$

From the first of these equations

$$p'(N) = \alpha_2 \bar{t}'(N). \quad (5.3.2)$$

Since adding a vehicle changes traffic conditions only at the end of the rush hour,

$$\bar{t}'(N) = \frac{1}{q(\bar{t}(N))}; \quad (5.3.3)$$

in words, adding a vehicle increases the length of the rush hour by the reciprocal of the arrival rate. Thus,

$$p'(N) = \frac{\alpha_2}{q(\bar{t}(N))} \quad (5.3.4)$$

and⁸

$$\begin{aligned}
p''(N) &= -\frac{\alpha_2 q'(\bar{t}(N)) \bar{t}'(N)}{q(\bar{t}(N))^2} \\
&= -\frac{\alpha_2 q'(\bar{t}(N))}{q(\bar{t}(N))^3}
\end{aligned} \tag{5.3.5}$$

Since the arrival rate is increasing over the rush hour, the trip price function is concave.

Total variable trip costs are $Np(N)$. Thus, marginal variable trip cost as a function of N is

$$\begin{aligned}
MVTC(N) &= p(N) + Np'(N) \\
&= \bar{t}(N) - t_f(N) - 1 + \frac{\alpha_2 N}{q(\bar{t}(N))}.
\end{aligned} \tag{5.3.6}$$

Since trip price and marginal variable trip cost are independent of departure time, the congestion externality cost too is independent of departure time, and equals $\frac{\alpha_2 N}{q(\bar{t}(N))}$. Consider adding the marginal vehicle at the end of the rush hour. Because this additional vehicle has no effect on traffic conditions for inframarginal vehicles, it does not affect their travel time cost, but instead increases each vehicle's schedule delay by $\frac{1}{q(\bar{t}(N))}$ at a social cost of $\frac{\alpha_2 N}{q(\bar{t}(N))}$. For the same reason, marginal schedule delay cost is $\frac{\alpha_2 N}{q(\bar{t}(N))}$ and marginal variable travel time cost is $p(N)$. Since marginal variable travel time cost is $p(N)$ and marginal schedule delay cost is $Np'(N)$, and since $p(N)$ is concave, for each level of population marginal variable travel time cost exceeds marginal schedule delay cost. And since marginal variable travel time cost equals trip price, and since marginal schedule delay cost equals the congestion externality cost, at each level of population trip price exceeds the congestion externality cost.

⁸For some pairs of N and α_2 , satisfaction of the trip-timing condition requires the development of a queue. One may distinguish two different trip cost régimes, according to whether the last person to depart does not face a queue (régime 1 - low congestion) or faces a queue (régime 2 - high congestion). In α_2 - N space, the boundary between the two régimes is negatively sloped, with high congestion occurring above the boundary and low congestion below it (since an increase in α_2 causes more weight to be placed on schedule delay, which compresses the rush hour).

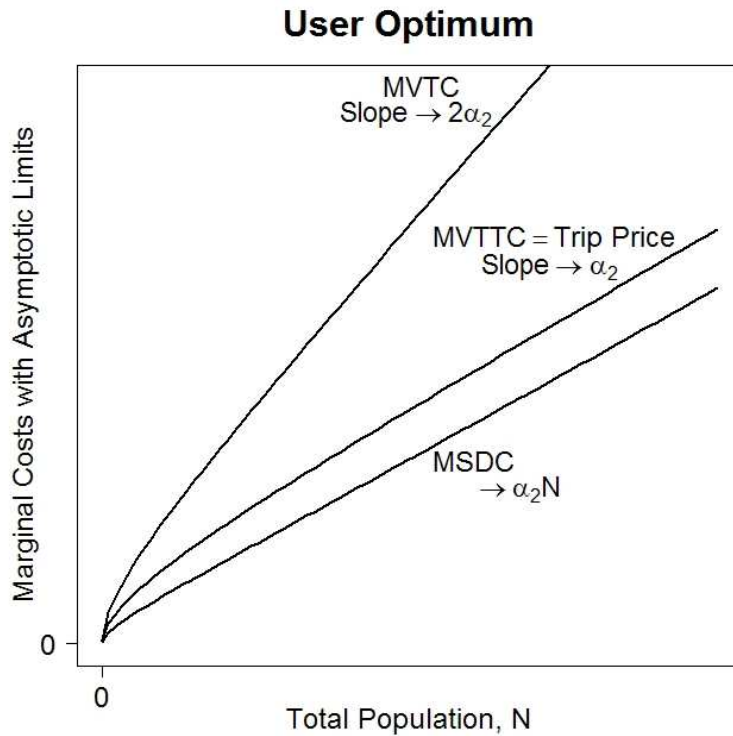


Figure 5.3: Marginal costs as functions of population for the user optimum, with $\alpha_2 = 0.5$.

Figure 5.3 is analogous to Figure 5.1 for the social optimum, except that it adds the trip price function. The marginal variable trip cost function is the vertical sum of the marginal schedule delay cost and marginal variable travel time cost functions, and the trip price function coincides with the marginal variable travel time cost function. All four functions equal zero at zero population. In the limit as N approaches infinity, the arrival rate approaches 1. The marginal schedule delay function approaches $\alpha_2 N$, the slope of the price function (= travel time cost function) approaches α_2 , and the slope of the marginal variable trip cost function approaches $2\alpha_2$.

5.4 Comparison of the Social Optimum and User Optimum

Figure 5.4 displays cumulative departures and arrivals, for both the social optimum and the no-toll equilibrium, with $N = 0.8$ and $\alpha_2 = 0.5$. Although $N = 8$ is consistent with the level

of rush-hour congestion found in large metropolitan areas that are moderately congested by international standards⁹, the qualitative features of the graph can be better viewed with smaller values of N . $\alpha_2 = 0.5$ is consistent with the empirical evidence. The curves for the social optimum are shown with solid lines, those for the no-toll equilibrium with dashed lines. The shapes of the two cumulative arrival curves are similar, though the rush hour is somewhat longer in the social optimum than in the no-toll equilibrium, resulting in higher total schedule delay in the social optimum than in the no-toll equilibrium. The cumulative departure schedules, however, have different shapes. In the social optimum, the schedule has a sigmoid shape, while in the no-toll equilibrium it is convex. Total travel times are considerably lower in the social optimum than in the no-toll equilibrium, partly because travel on the road is more congested in the no-toll equilibrium and partly because queuing occurs in the no-toll equilibrium but not in the social optimum.

Figure 5.5 superimposes Figures 5.1 and 5.3. The solid lines are for the social optimum and the dashed lines for the user optimum. Five points bear note.

1. The marginal schedule delay cost function for the social optimum lies above that for the user optimum. This occurs because, at each level of population, the arrival rate at \bar{t} is lower in the social optimum than in the user optimum.
2. The marginal variable travel time cost function for the social optimum lies below that for the user optimum. For small N , this arises because, at each level of population, travel is less congested in the social optimum than in the user optimum. Furthermore, for large N , there is no queuing in the social optimum, but there is in the user optimum.
3. The marginal variable trip cost function for the social optimum lies below that for the

⁹Because the paper is already long, we have avoided providing numerical examples. However, it will be useful to illustrate how the model can be calibrated. Consider a metropolitan area in a poorer country, where infrastructure is low relative to traffic volume over the rush hour. $\frac{N}{q_m}$ is how long the rush hour would be if traffic were at capacity flow for the entire rush hour, and provides an exogenous measure of infrastructure capacity relative to population. Suppose this equals 2.0 hours. Suppose too that $\frac{l}{v_0} = .25$ hours (the average trip would take 15 minutes at free-flow speed). Then, in scaled units the population is $N_{\text{Scaled}} = \frac{N}{q_m \frac{l}{v_0}} = \frac{2.0}{.25} = 8$.

Cumulative Inflow/Outflow Curves

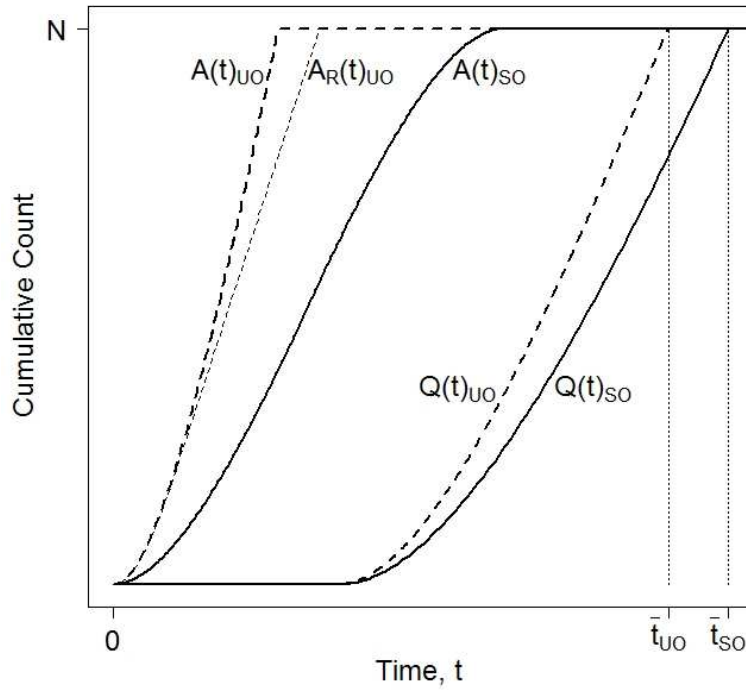


Figure 5.4: Cumulative inflow and outflow curves for the social optimum (solid lines) and user optimum (dashed lines), with $N = 0.8$ and $\alpha_2 = 0.5$. In the user optimum a queue develops when inflow into the corridor exceeds capacity, so that $A(t)_{UO}$ is the cumulative corridor inflow curve, $A_R(t)_{UO}$ is the cumulative road inflow curve, and the horizontal distance between these curves is the queueing time.

user optimum.

4. At a given level of population, the deadweight loss in the user optimum compared to the social optimum, due to the underpricing of congestion in the user optimum, equals the area between the two marginal variable trip cost functions up to that level of population.
5. In the decentralized social optimum, the trip price equals $MVTC_{SO}$, while in the no-toll equilibrium it equals $MVTTC_{UO}$. Since the $MVTC_{SO}$ curve lies above the $MVTTC_{UO}$ curve for all levels of N , the toll revenue collected from the optimal time-varying toll exceeds the efficiency gain from applying it¹⁰.

¹⁰The revenue collected from the optimal time-varying toll can be calculated from the relationship for the

Social and User Optimum

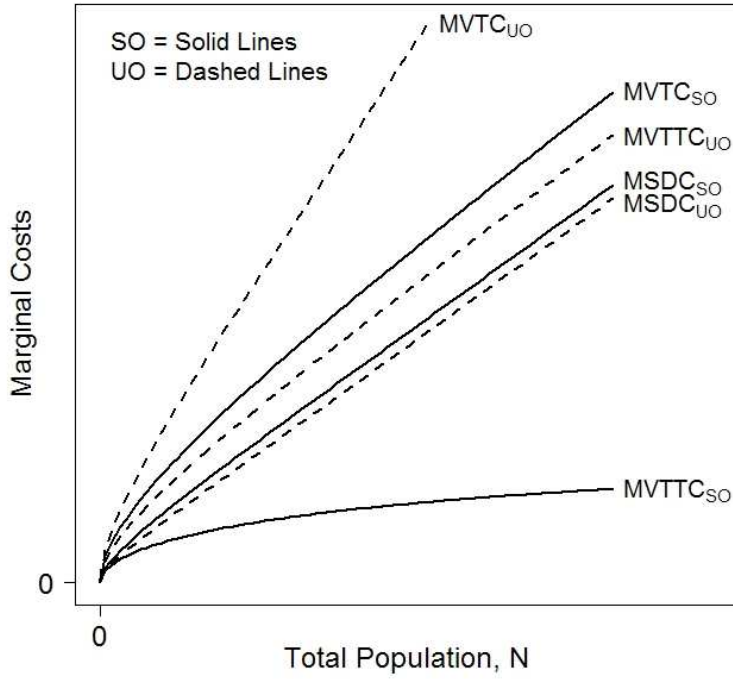


Figure 5.5: Marginal costs for the social optimum (solid lines) superimposed with the marginal costs for the user optimum (dashed lines), as functions of population, with $\alpha_2 = 0.5$.

5.5 Comparison of the Single-Entry Corridor Model to the Bottleneck Model

The basic bottleneck model, with identical individuals, a common desired arrival time, and no fixed component of trip cost, is starkly simple. All congestion takes the form of queuing behind a bottleneck of fixed flow capacity, and the arrival rate equals bottleneck capacity over the arrival interval in both the social optimum and user optimum. In the social optimum, variable travel time costs are zero, and marginal schedule delay cost (and hence marginal

decentralized social optimum that toll revenue, R , plus total variable trip costs equals trip price times population. Thus, for the level of population N' , $R = MVTC_{SO}(N')N' - \int_0^{N'} MVTC_{SO}(N) dN$. The efficiency gain from applying the optimal time-varying toll, G , equals the total variable trip cost in the no-toll equilibrium minus total variable trip cost in the social optimum: $G = MVTT_{C_{UO}}(N')N' - \int_0^{N'} MVTC_{SO}(N) dN$. Thus, $R - G = [MVTC_{SO}(N') - MVTT_{C_{UO}}(N')]N'$.

variable trip cost) is linear in population. In the user optimum, total variable travel time cost equals total schedule delay cost. The marginal schedule delay cost curve is the same as in the social optimum and coincides with the marginal variable travel time cost curve, so that the marginal variable trip cost curve has double the slope of both. In a decentralized environment, imposition of the optimal time-varying toll has no effect on the length of the rush hour or on total schedule delay cost but completely eliminates variable travel time cost, so that the deadweight loss in the user optimum due to unpriced congestion equals total variable travel time cost in the user optimum. Since the optimal time-varying toll simply replaces the user optimum's variable travel time costs - queuing costs - the revenue raised from the optimal time-varying total equals the user optimum's total variable travel time costs and also the deadweight loss in the user optimum due to unpriced congestion. Thus, imposition of the optimal time-varying toll would benefit users as long as part of the revenue it generates is used to their benefit.

The single-entry corridor model takes a step towards realism by treating LWR flow congestion. Like the bottleneck, the road in the single-entry corridor has a fixed flow capacity; but unlike the bottleneck, the road becomes congested at flow rates below capacity. In a decentralized environment, imposition of the optimal time-varying toll reduces congestion but does not eliminate it and causes the rush hour to lengthen. In the social optimum, marginal schedule delay cost, marginal variable travel time cost, and marginal variable trip cost, are all concave functions of population. Since there is neither hypercongestion nor queuing in the social optimum, marginal variable travel time cost has an upper bound, but marginal schedule delay cost and marginal variable trip cost do not. In the user optimum too, marginal schedule delay cost, marginal variable travel time cost, and marginal variable trip cost, are all concave functions of population. Since there is queuing in the user optimum for sufficiently large N , although no hypercongestion, marginal variable travel time cost has no upper bound. The trip price function coincides with the marginal variable travel time cost function, the congestion externality cost function coincides with the marginal sched-

ule delay cost function, and the marginal variable travel time cost function lies above the marginal schedule delay cost function. As in the bottleneck model, the time-varying toll rises monotonically from zero at the beginning of the departure interval to marginal variable trip cost at the end, but is convex in departure time, whereas it is linear in departure time in the bottleneck model. Imposition of the optimal time-varying toll alters the departure function, as in the bottleneck model, but unlike the bottleneck model also alters the arrival function.

The single-entry corridor model provides a more realistic treatment of congestion than the bottleneck model, but this comes at the cost of increased complexity and/or the need to resort to numerical solution. Which model is preferable depends on context. The bottleneck model has the advantage that its simplicity admits numerous analytical extensions, but this same simplicity leads to some unrealistic properties that can be misleading in policy analysis. Assuming bottleneck congestion facilitates the computation of dynamic network equilibrium but treating each link as being subject to LWR flow congestion should lead to more accurate results.

Like the basic bottleneck model, the single-entry corridor model treats demand as being inelastic. And as with the basic bottleneck model, the extension to treat price-sensitive demand would be straightforward. Like the basic bottleneck model, the single-entry corridor model treats the desired arrival time distribution as exogenous, whereas it should be endogenous and derived from employers' profit-maximizing decisions concerning employee start time. In assuming that no vehicle can lower its trip cost by altering its departure time, both the basic bottleneck model and the single-entry corridor model assume that trip-timing decisions are based on perfect information.

Despite their differences, the single-entry corridor model is far more similar to the bottleneck model than either is to the static model of congestion. In the single-entry corridor and the bottleneck model with (as assumed) inelastic demand, tolling is effective through altering the timing of departures over the rush hour. In the static model of congestion,

in contrast, tolling is effective through altering the number of vehicles. Empirically, since demand for commuting trips is highly inelastic, it appears that the welfare gains from altering the timing of departures are quantitatively more important than those from reducing demand. Furthermore, through ignoring the trip-timing margin of adjustment, application of the standard model has likely resulted in overstating the benefits from reducing overall traffic volume.

6 Concluding Remarks

6.1 Directions for Future Research

The basic bottleneck model has been extended in numerous ways. Some of these extensions would be straightforward to undertake for the current model, such as allowing for price-sensitive demand, determining optimal capacity, treating users who differ continuously in unit travel time and schedule delay costs, and considering routes in parallel. Others would not be straightforward. The first is to treat late, as well as early, arrival. The difficulty here derives from the analytical complexity of dealing with the discontinuity in the departure rate at the boundary between early and late arrivals. The second is to treat a road of non-uniform width. The third is to treat merges. Merges occur along a traffic corridor with more than one entry point, and also on networks in which two or more directional links meet at a common node. Once the non-uniform road width and merge problems have been solved, it should be possible to determine the SO and UO with LWR flow congestion on a general corridor and a general network.

An undesirable property of the current model is that travel is not congested in the UO. But congested travel is ubiquitous. We strongly suspect that congested travel will emerge in the UO but not in the SO once the model is extended to treat either non-uniform road width or merges.

The model assumes that commuters know perfectly how congestion evolves over the rush

hour. All congestion is recurrent, and all commuters recognize that it is recurrent. But in fact much congestion is non-recurrent due to variable weather conditions, traffic accidents, and road construction, about which commuters are imperfectly informed. Some work has been done on non-recurrent congestion in the context of the bottleneck model. DePalma is currently working on extending this paper's model to treat randomly occurring incidents along the road. How they will affect the SO and UO will depend on how well informed commuters are of their occurrence. However well informed they are, in both the SO and UO, incidents will lead to congested travel.

6.2 Conclusion

Because of its simplicity, the bottleneck model has been widely employed in theoretical analyses of rush-hour traffic congestion. But this simplicity is attained at the cost of providing an unrealistic treatment of the congestion technology. One wonders which of the bottleneck model's properties are robust, and which derive from the simplicity of the assumed congestion technology. Newell took a step towards remedying this deficiency by replacing the bottleneck with a single-entry corridor of uniform width that is subject to LWR flow congestion, for which the bottleneck is a limiting case. His paper has been rather overlooked by the literature, probably because of its density. This paper considered a special case of Newell's model in which local velocity is a negative linear function of local density, and all commuters have a common desired arrival time at the central business district. These simplifying assumptions permitted complete, closed-form solutions for the social optimum and an analytical solution for the user optimum departure rate. Providing detailed derivations and exploring the model's economic properties added insight into rush-hour traffic dynamics in the social optimum and user optimum with this form of congestion, and into how the dynamics differ from those of the bottleneck model.

References

- Arnott, R. and de Palma, A. and Lindsey, R. (1990). Economics of a bottleneck. *Journal of Urban Economics*, 27(1), 111–130.
- Arnott, R. and de Palma, A. and Lindsey, R. (1993). A structural model of peak-period congestion: a traffic bottleneck with elastic demand. *The American Economic Review*, 83(1), 161–179.
- Arnott, R. and DePalma, E. (2010). The corridor problem: preliminary results on the no-toll equilibrium. *Transportation Research Part B*, in press.
- Daganzo, C. (1994) A finite difference approximation of the kinematic wave model of traffic flow. *Transportation Research Part B*, 29(4), 261–276
- Daganzo, C. (1997) Fundamentals of transportation and traffic operations. Elsevier Science, New York, NY
- Lago, A. and Daganzo, C. (2007) Spillovers, merging traffic and the morning commute. *Transportation Research Part B*, 41(6), 670–683.
- Lighthill, M.H. and Whitham, G.B. (1955). On kinematic waves II: a theory of traffic flow on long crowded roads. *Proc. Roy. Soc. (Lond.)*, 229(1178), 317–345.
- Mattheij, R. and Rienstra, J.H.M. (2005) Partial differential equations: modeling, analysis, computation. SIAM, Philadelphia, PA
- Newell, G.F. (1988). Traffic flow in the morning commute. *Transportation Science*, 22(1), 47–58.
- Richards, P.I. (1956). Shock waves on the highways. *Operations Research*, 4(1), 42–51.
- Small, K. (1982). The scheduling of consumer activities: Work trips. *American Economic Review*, 72(3), 467–479.

Vickrey, W. (1969). Congestion theory and transport investment. *The American Economic Review*, 59(2), 251–260.

Wong, S.C. and Wong, G.C.K. (2002). An analytical shock-fitting algorithm for LWR kinematic wave model embedded with linear speed-density relationship. *Transportation Research Part B*, 36(8), 683–706.

Glossary

SO	Social Optimum
UO	User Optimum
CBD	Central Business District
x, t	Space and time coordinates
l	Spatial location of the CBD
$a(t), A(t)$	Corridor inflow and cumulative inflow rates
$a_R(t), A_R(t)$	Road inflow and cumulative inflow rates
$q(t), Q(t)$	Corridor outflow and cumulative outflow rates (at $x = l$)
N	Size of population
t_f, t_R	Time of final departures into the corridor and road, respectively
\bar{t}	Time of final arrival at the CBD
$\tau(t)$	Travel time of a departure at time t (includes queueing time)
α_1, α_2	Per unit population costs of travel time and schedule delay
$C(t)$	(Per unit population) Trip cost for a departure at time t
TTC	Total Trip Cost (aggregate sum of trip costs for entire population)
$k(x, t), v(x, t), q(x, t)$	Density, velocity and flow rate at spacetime point (x, t)
v_0	Free-flow velocity
k_j	Jam density
q_m	Capacity flow
k_m	Density at which capacity flow is reached
w	Reciprocal of wave velocity normalized by v_0 , $w = \frac{v_0}{q'(k)}$
k_l, k_r	Densities to the left and right of a shock wave path
q_l, q_r	Flow rates to the left and right of a shock wave path
q_c	Constant inflow rate
w_c	Characteristic slope for a flow rate of q_c

v_c	Velocity for a flow rate of q_c
t_c	Departure time for arrival at time w_c under constant velocity, v_c
t_d, t_a	Departure and arrival times, respectively
(x_0, t_0)	Spacetime intersection point of a trajectory with a rarefaction wave boundary
A	Arbitrary constant of integration in an ordinary differential equation
TSD	Total Schedule Delay (aggregate sum of schedule delays for entire population)
TTT	Total Travel Time (aggregate sum of travel times for entire population)
$q^*(w)$	Nondimensional outflow rate of maximal growth
$Q^*(w)$	Nondimensional cumulative outflow of maximal growth
t'_0	Time of the first arrival in the SO
w_0	Characteristic slope at the CBD at time t'_0
TT	Trip-Timing Condition
σ	Shorthand notation for $\frac{1}{1-\alpha_2}$ in the UO
$g(a(t))$	Shorthand notation for $\frac{1}{\sqrt{1-a(t)}} - 1$ in the UO
a_f	Inflow rate at time t_f
t_Q	Time at which a queue develops in the UO
N_c	Critical population value such that a queue develops if $N > N_c$ in the UO
T	Total (Section 5)
A	Average (Section 5)
M	Marginal (Section 5)
F	Fixed (Section 5)
V	Variable (Section 5)
C	Cost (Section 5)
E	Elasticity (Section 5)
$\tau(t_d)$	Toll at departure time t_d (Section 5)
$p(N)$	Trip price in excess of free-flow travel time cost (Section 5)

Appendix

Greenshields' Relation

In (A-1) we summarize the relationships for Greenshields' Relation between k , v and q assuming ordinary (uncongested) flow, $k \leq k_m$ (see section 2.2):

$$\frac{v}{v_0} = 1 - \frac{k}{2k_m} \Leftrightarrow \frac{k}{k_m} = 2 \left(1 - \frac{v}{v_0} \right)$$

$$\frac{q}{q_m} = 2 \frac{k}{k_m} \left[1 - \frac{k}{2k_m} \right] \Leftrightarrow \frac{k}{k_m} = 1 - \sqrt{1 - \frac{q}{q_m}} \tag{A-1}$$

$$\frac{q}{q_m} = 4 \frac{v}{v_0} \left(1 - \frac{v}{v_0} \right) \Leftrightarrow \frac{v}{v_0} = \frac{1}{2} \left[1 + \sqrt{1 - \frac{q}{q_m}} \right]$$

$$k_m = \frac{1}{2}k_j, \quad q_m = \frac{1}{2}v_0k_m, \quad v_m = \frac{1}{2}v_0.$$